Nuclear-reaction theory as a research tool for innovative radioisotope production in nuclear medicine.

Canton L. INFN - Sezione di Padova, Italy

Projects: REMIX, METRICS CS5 (Interdisciplinary); NUCSYS CS4

Collaboration: LNL, PD, PV, MI, FE, Arronax (Nantes), Ospedale Sacro Cuore Don Calabria (Negrar, Verona), IOV

Ricordo di Gianni Fiorentini
22 febbraio 1948 – 18 giugno 2022

Come direttore di Laboratorio LNL,
Gianni ha avuto un ruolo fondamentale e cruciale, fra le moltissime altre cose, nel portare la ricerca sui radiofarmaci nei laboratori LNL, e in particolare è la persona che mi ha incoraggiato ad impegnarmi in questa linea di ricerca.

Introduction to radionuclides for medicine

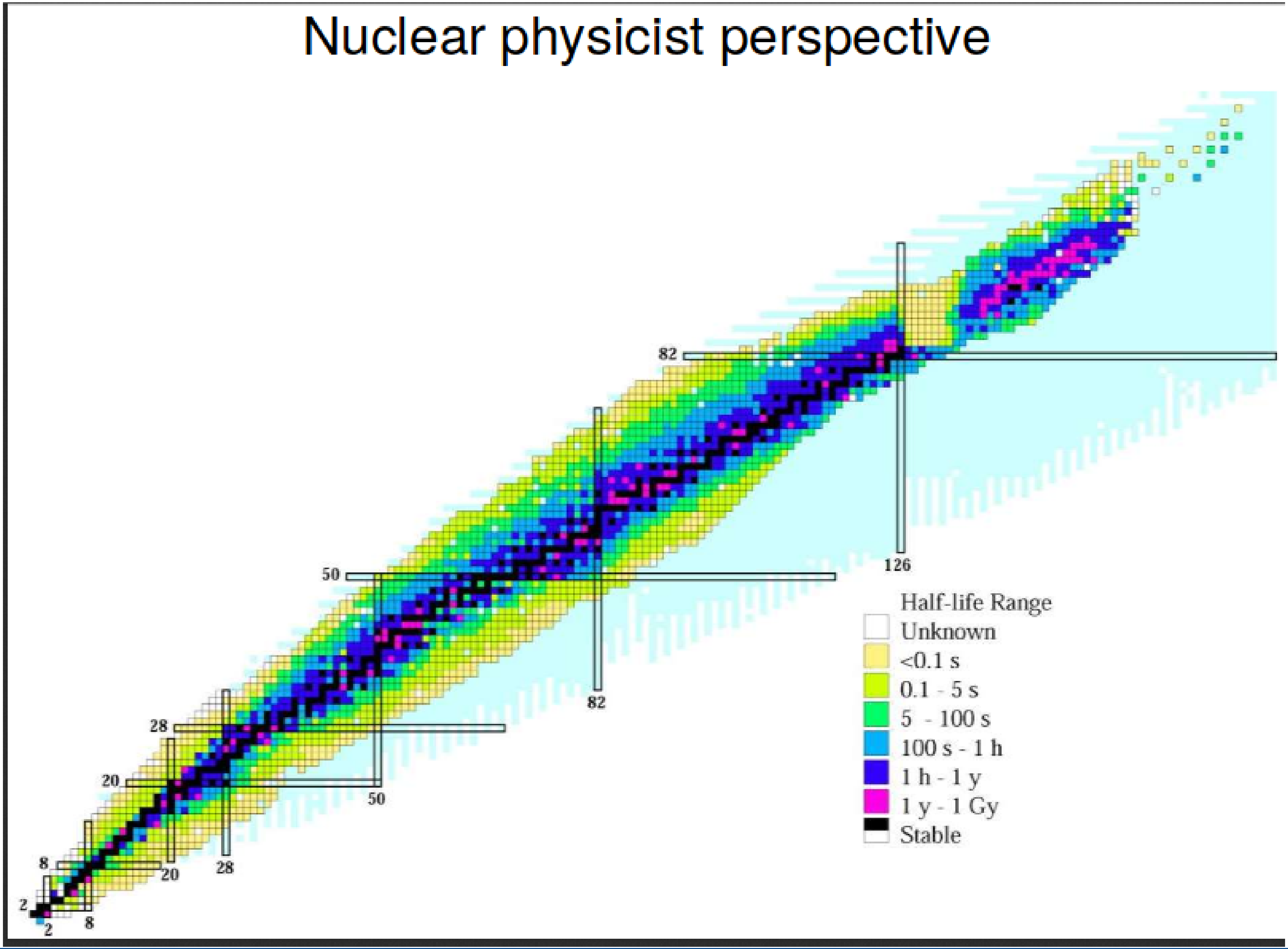

Introduction to radiotargeted therapy

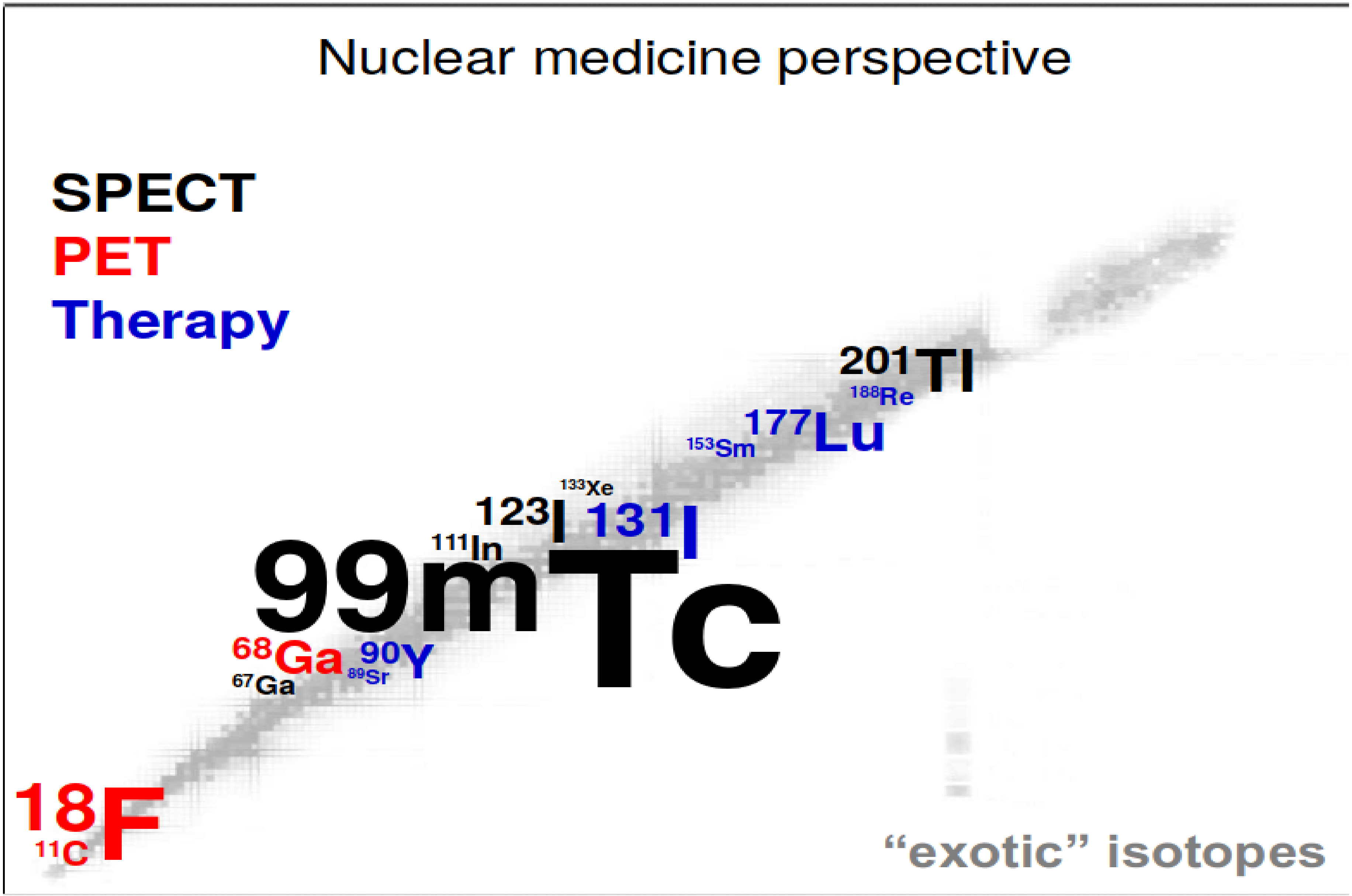

Introduction to radionuclides for medicine

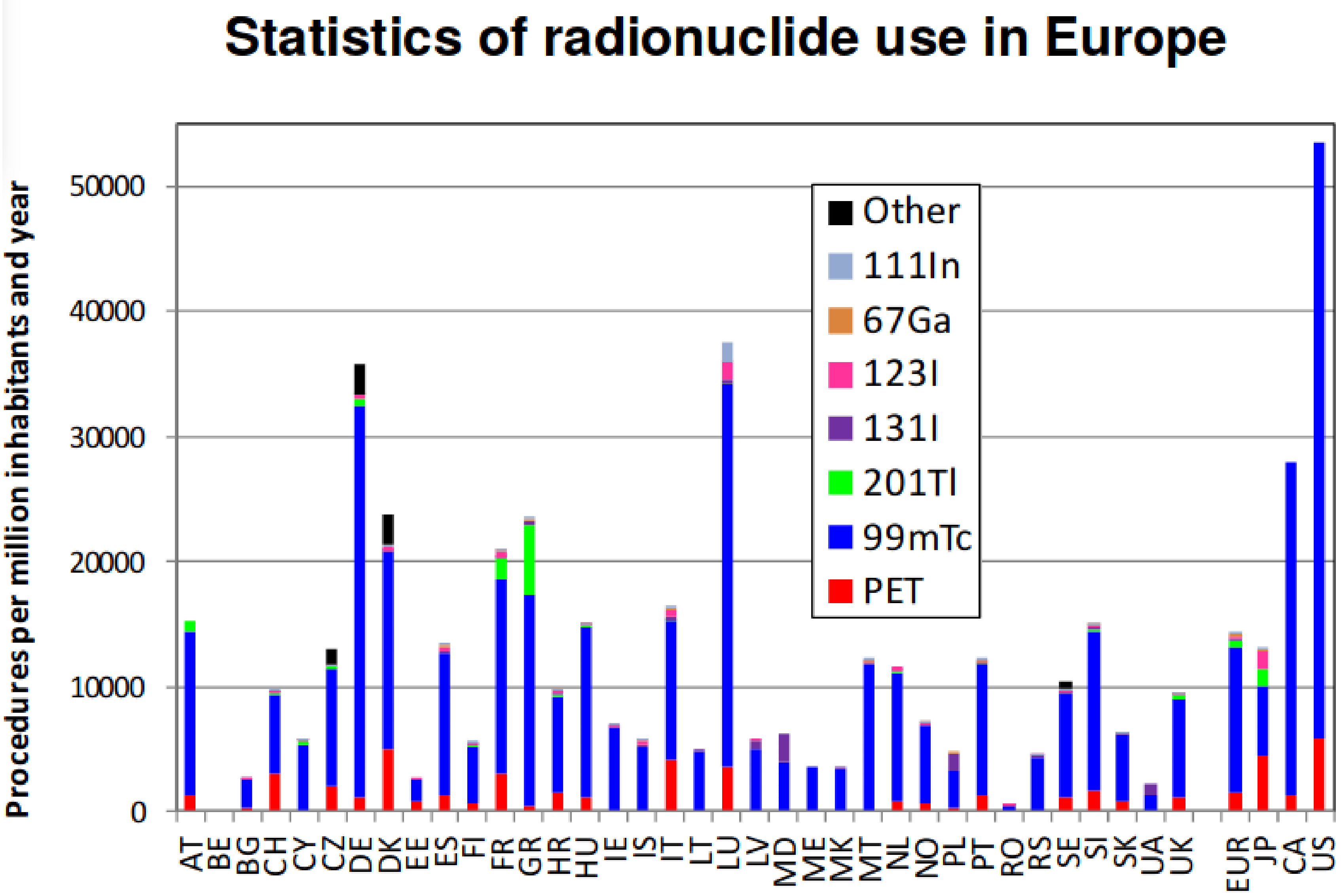

Use of diagnostic isotopes in Europe, USA, Canada and Japan

Introduction to radiotargeted therapy

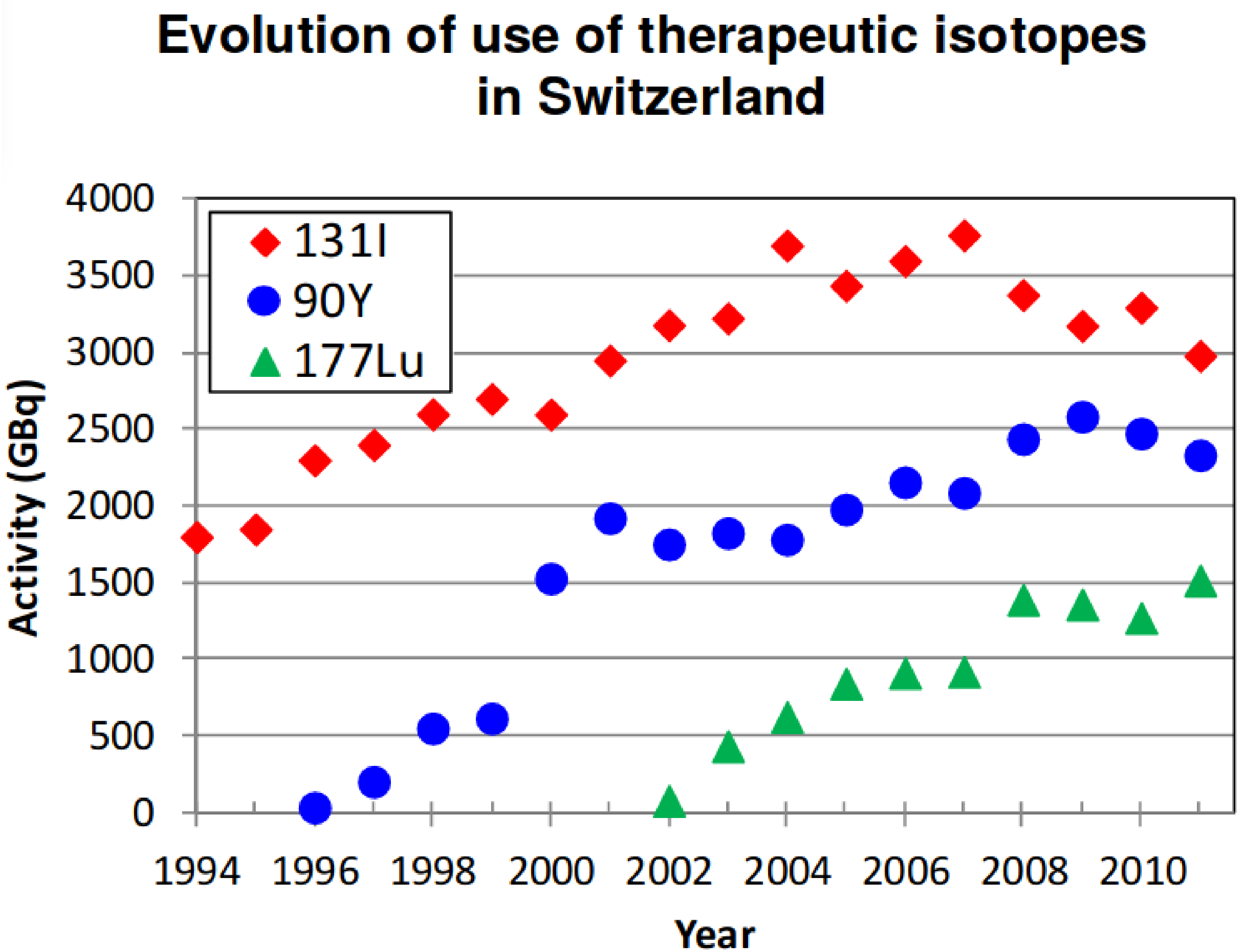

Introduction to radiotargeted therapy

Comparison of Cancer Therapies

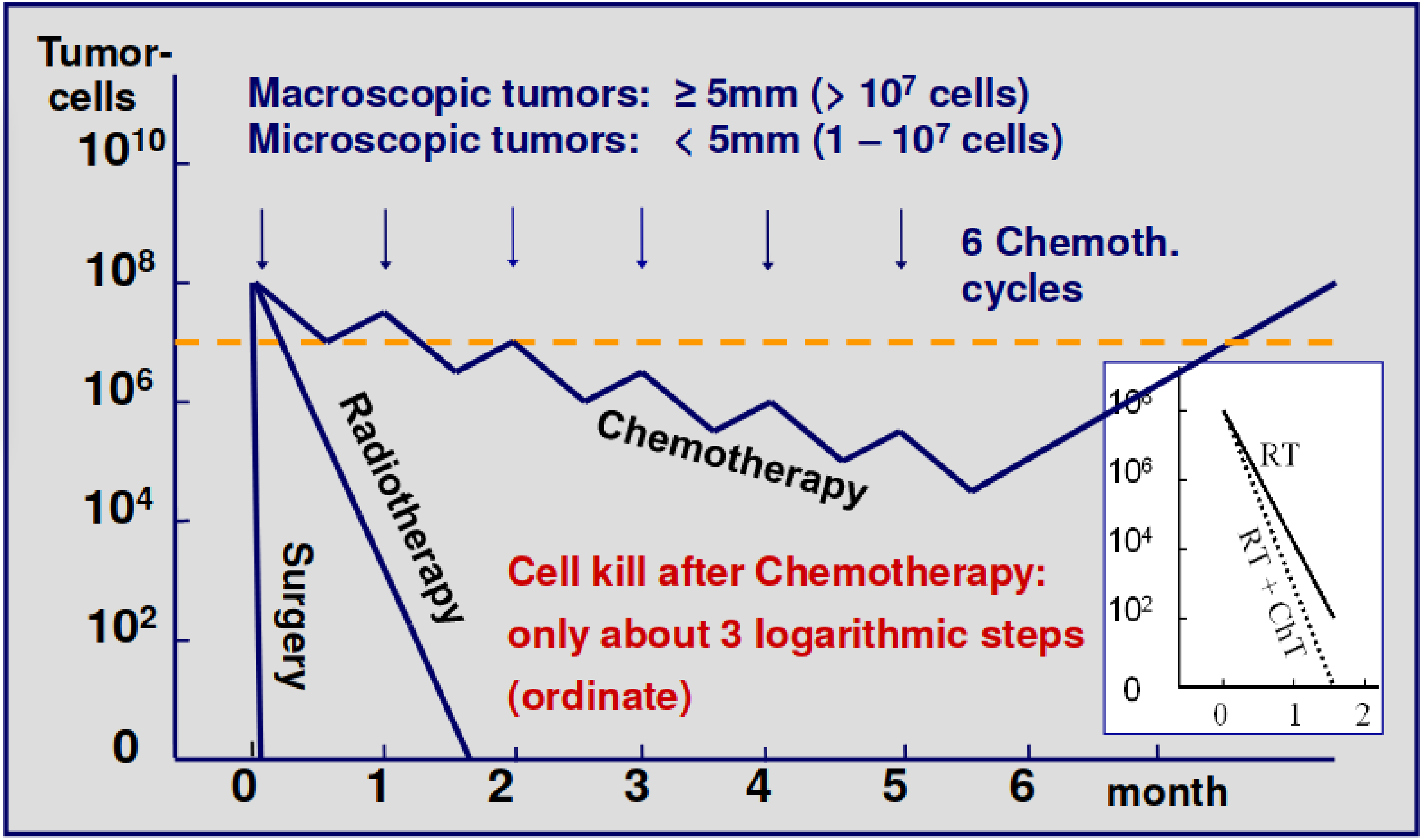

(Molls, TU München; according to Tannock: Lancet 1998, Nature 2006)

Introduction to radiotargeted therapy

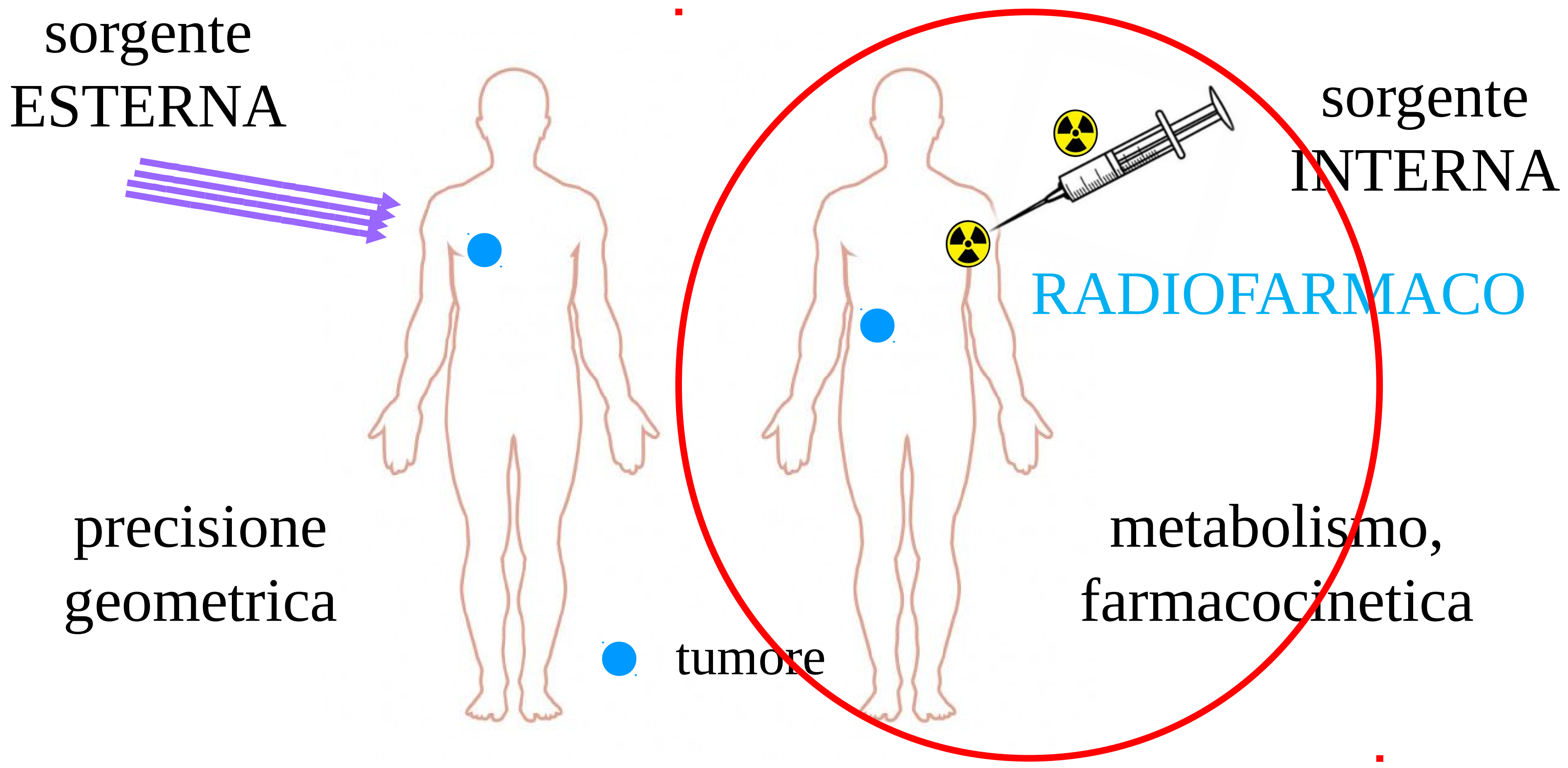

Introduction to radiotargeted therapy

Question: How to treat such patients?

Radiopharmaceticals – The Concept Simplified

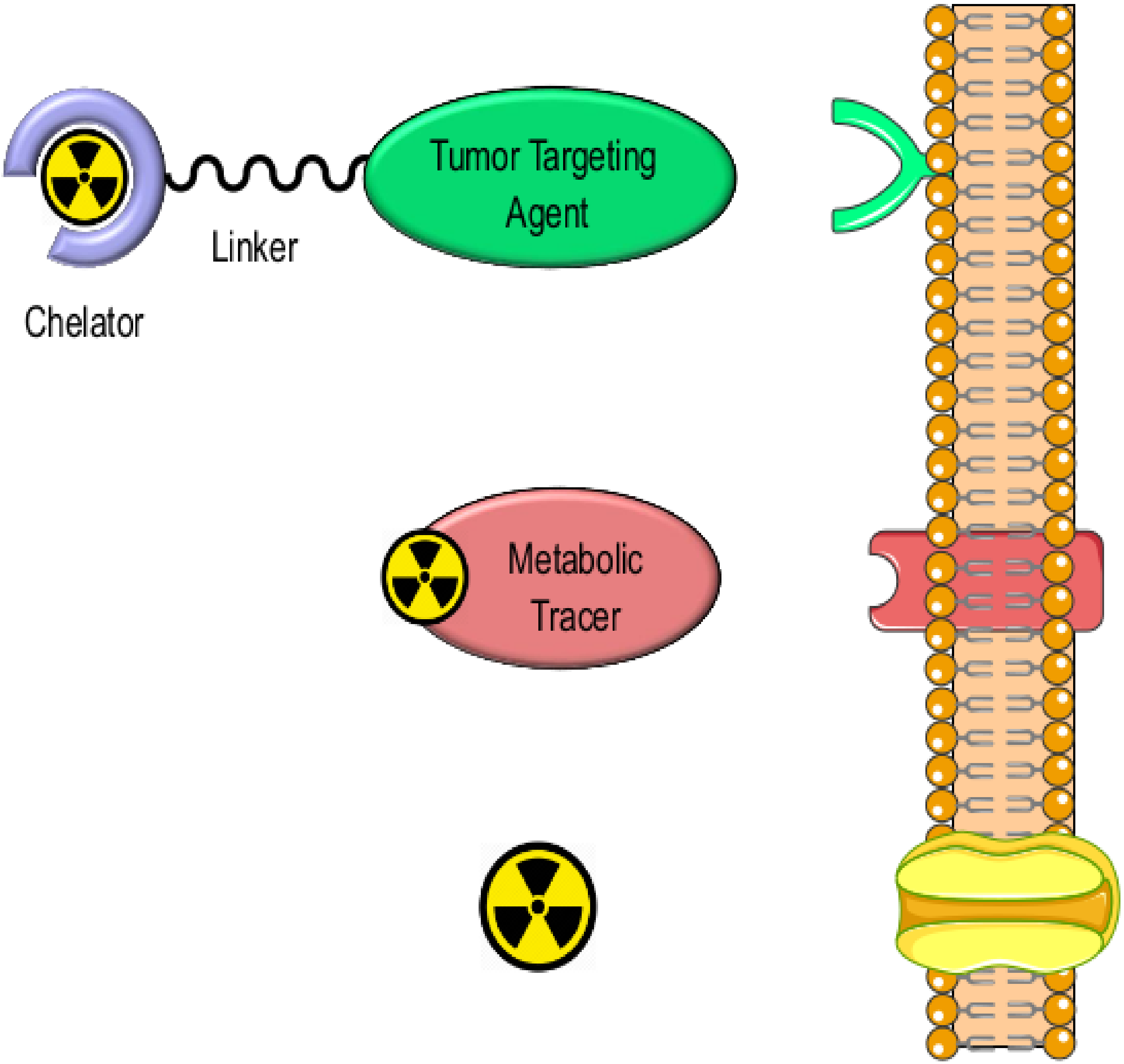

Examples:

^{68}Ga-DOTATATE
^{111}In-Octreotide
^{68}Ga-PSMA-11

^{18}F-Fluorodeoxy-Glucose (FDG)
^{18}F-Fluoro-ethyltyrosin (FLT)

^{123}I-Iodine
^{223}Ra-Radium

The principle of targeted therapies

- “attractive” vector > high uptake by the target
- transportable
- good in-vivo stability
- warriors “not visible”
- delayed uptake > suitable half-life
- limited space > high specific activity
- optimum arms
- specific

Introduction to radiotargeted therapy

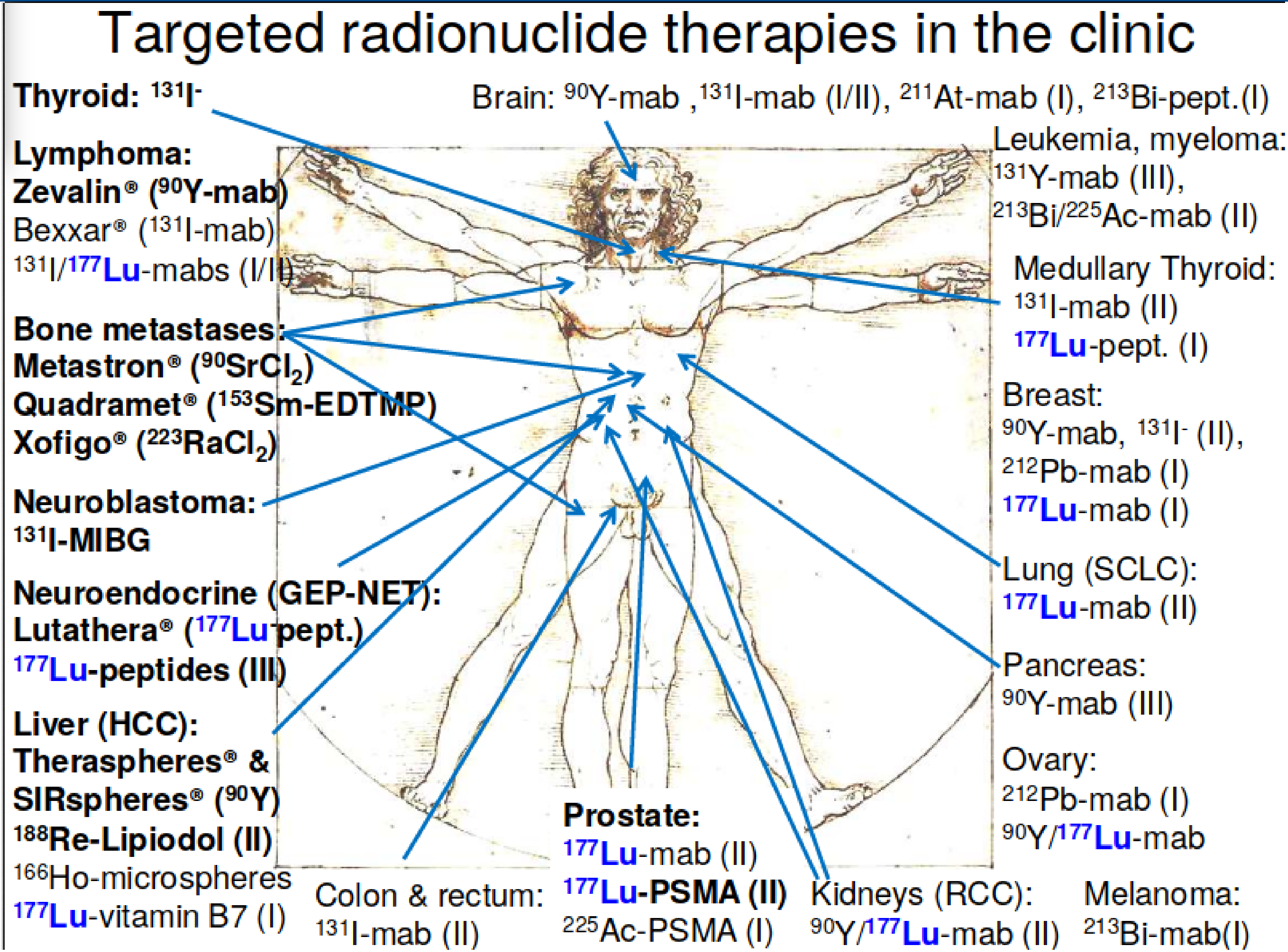

Introduction to radiotargeted therapy

^{99m}Tc
^{111}In
^{123}I
^{201}Tl
^{67}Ga
...

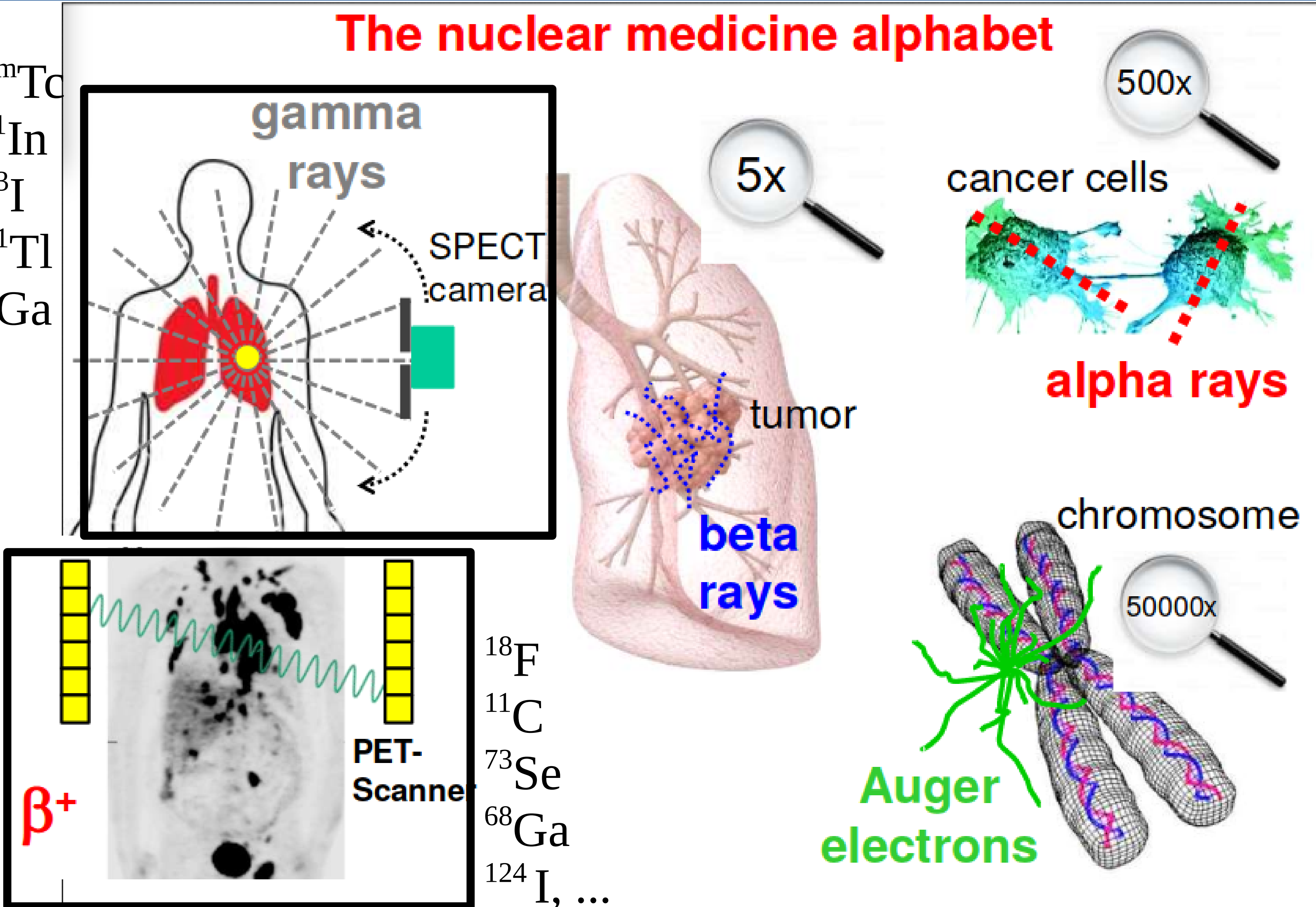

^{18}F
^{11}C
^{73}Se
^{68}Ga
^{124}I, ...

Range of therapeutic nuclides

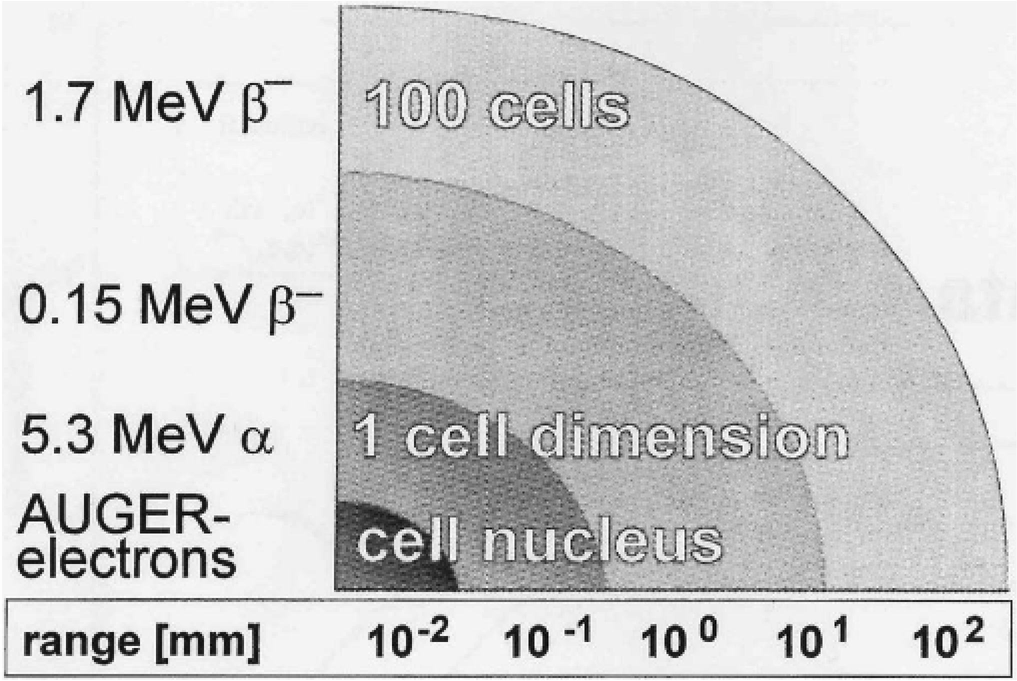

FIG. 1.1. Correlation between type and energy of corpuscular radiation, and the range in tissue

Range

Beta-	Alpha	Auger
Fino a 10 mm	Fino a 100 µm	~10 µm
(500 cellule)	(10 cellule)	(meno di una cellula)

Introduction to radiotargeted therapy

Lymphoma therapy: RITUXIMAB+^{177}Lu

E.B., 1941 (m): UPN 6

^{18}FDG PET | **^{177}Lu-Scan** | **^{18}FDG PET**

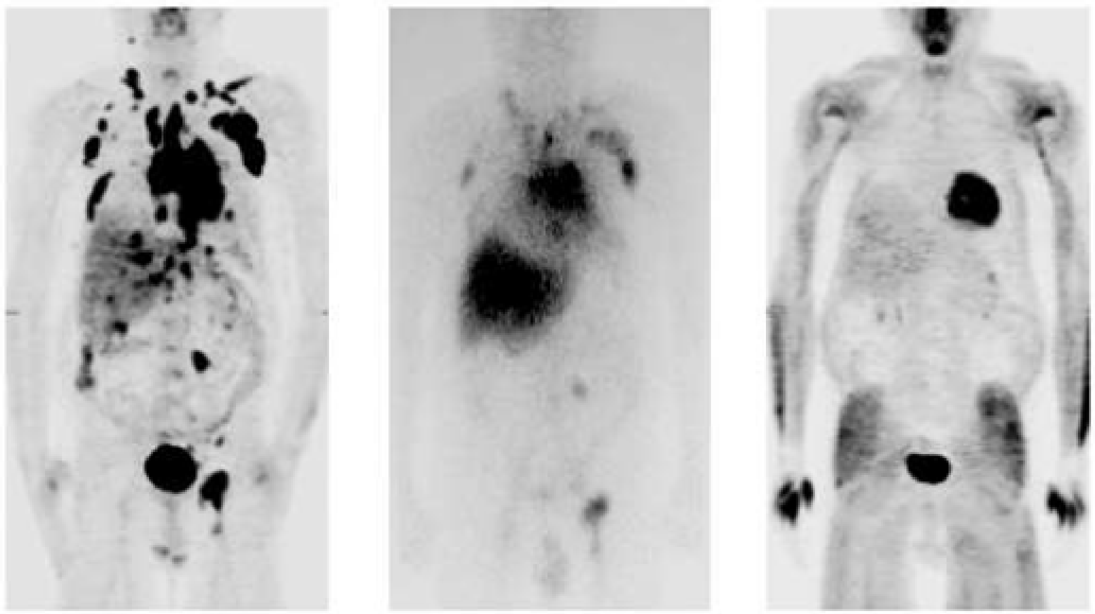

Still in CR

1.9.2002 | **13.9.2002** | **15.11.2002** | **15.9.2009**

F. Forrer et al., J Nucl Med 2013;54:1045.

University Hospital Basel, CH

Introduction to radiotargeted therapy

New Directions in Radionuclide Applications

JÜLICH FORSCHUNGSZENTRUM

Syed M Qaim,
Lecture IAEA, dec 2018

- **Theranostic approach**

  (combination of PET / Targeted therapy)

  $^{44}Sc/^{47}Sc$, $^{64}Cu/^{67}Cu$, $^{86}Y/^{90}Y$, etc.

- **Multimode imaging**

  (combination of PET/CT and PET/MRI)

- **Radioactive nanoparticles**

  Possible improvement in delivery of radionuclide to tumour

CUPRUM ..? 2023
COME INFN-LNL

PASTA, REMIX INFN-LNL

METRICS INFN-LNL

Continuous radionuclide research is underway.

Another view at the chemical elements

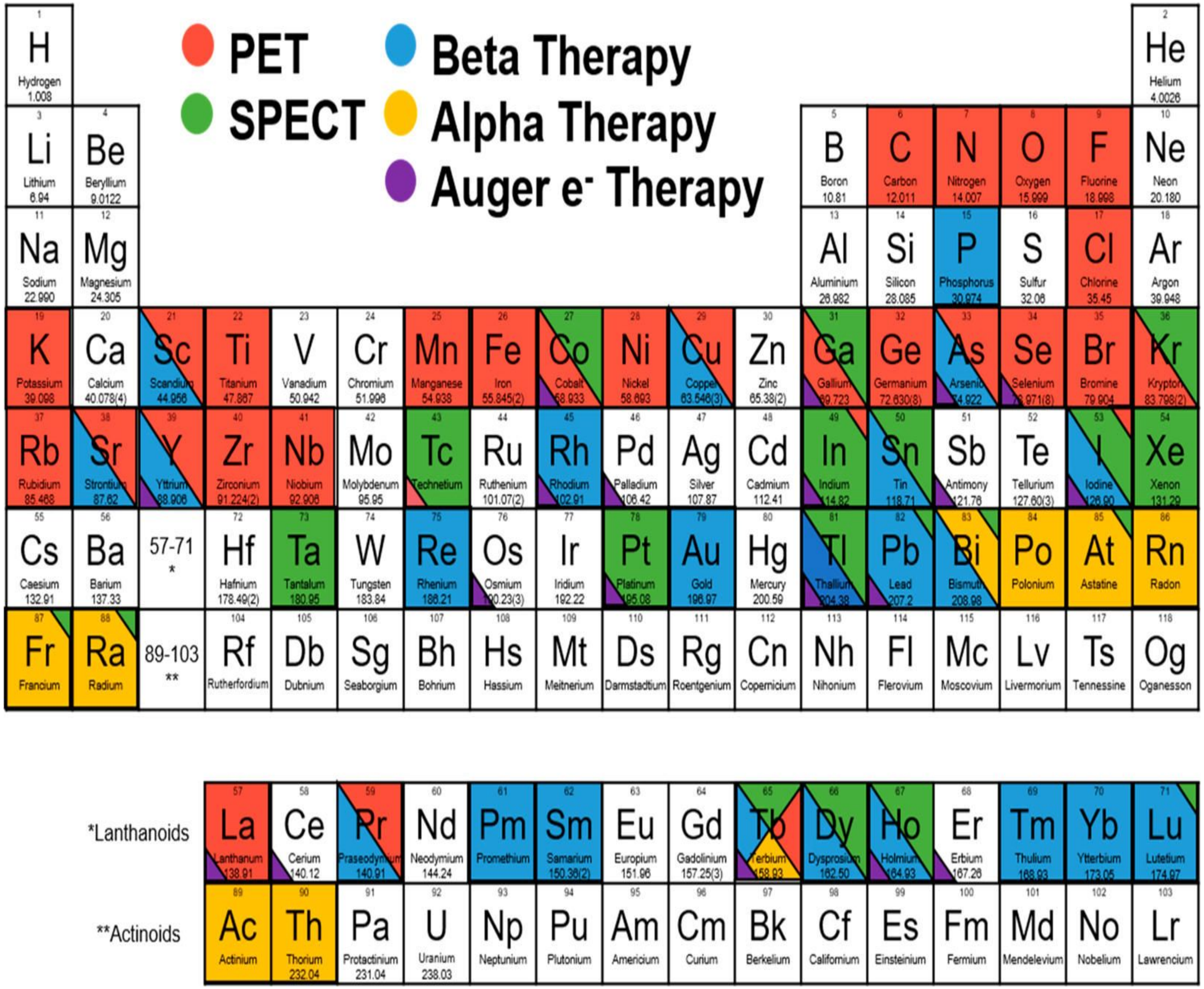

Another view at the chemical elements

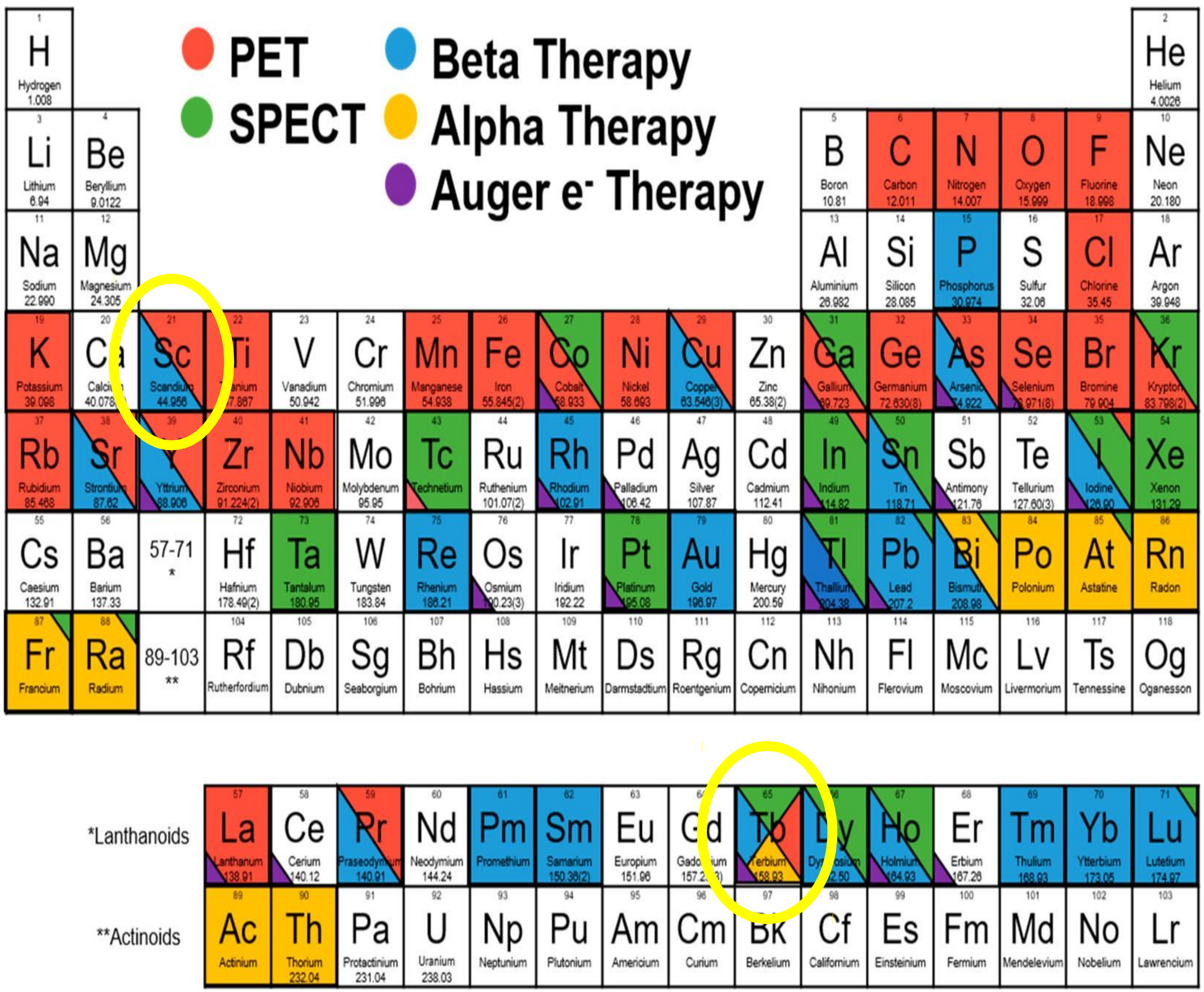

Introduction to radiotargeted therapy

t1/2 = 3,97 h;   t1/2 =3,35 d

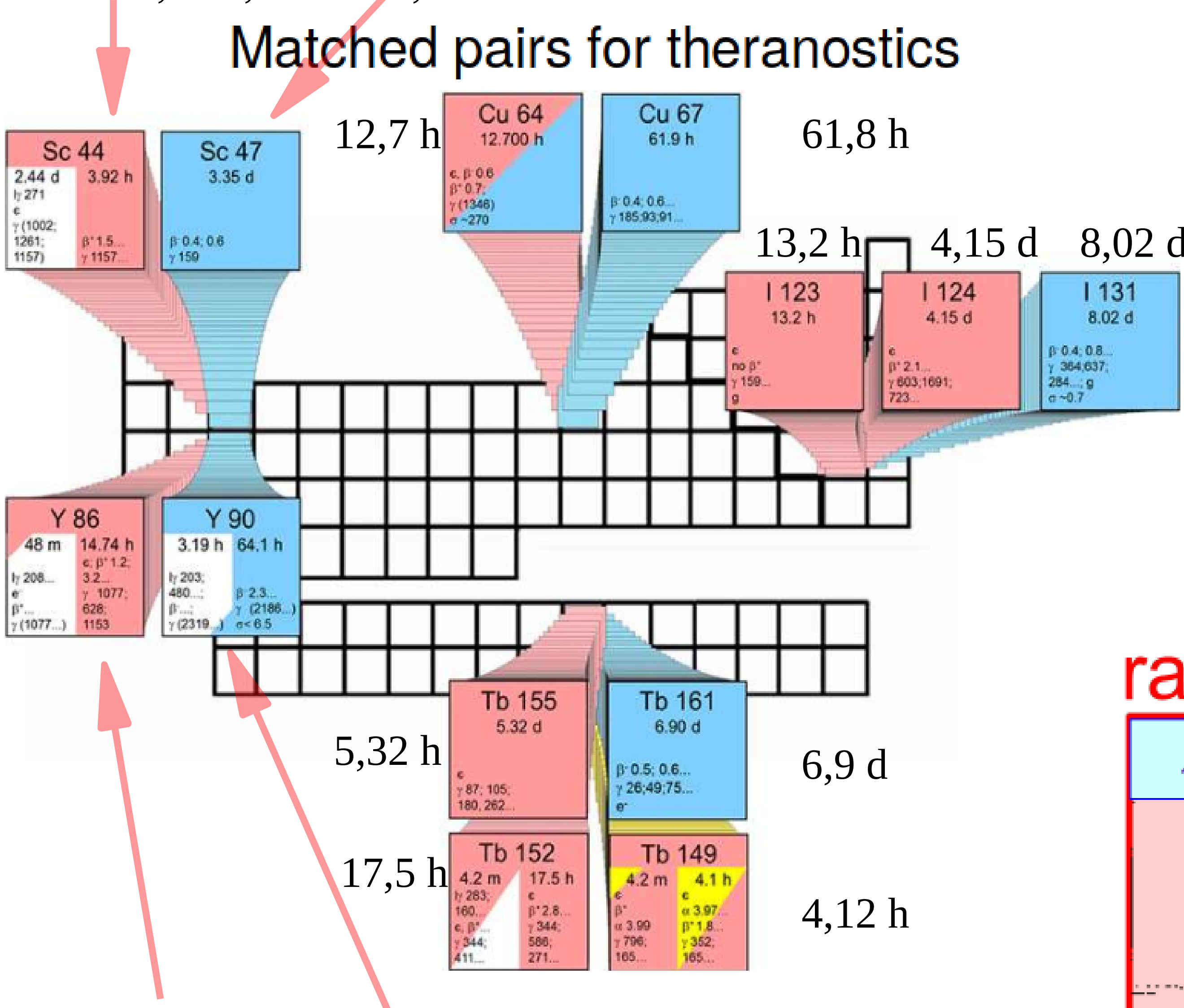

T1/2 = 14,74 h;   t1/2 =64,05 d

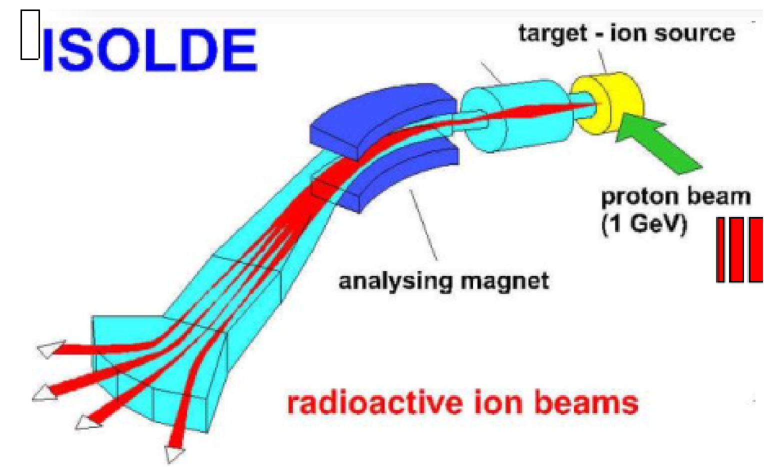

Spallation of Ta with high-energy protons following online mass separation

radioactive ion beams

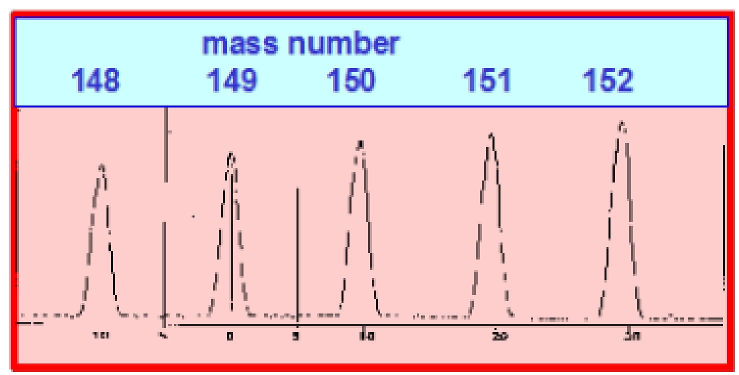

Therapeutic window

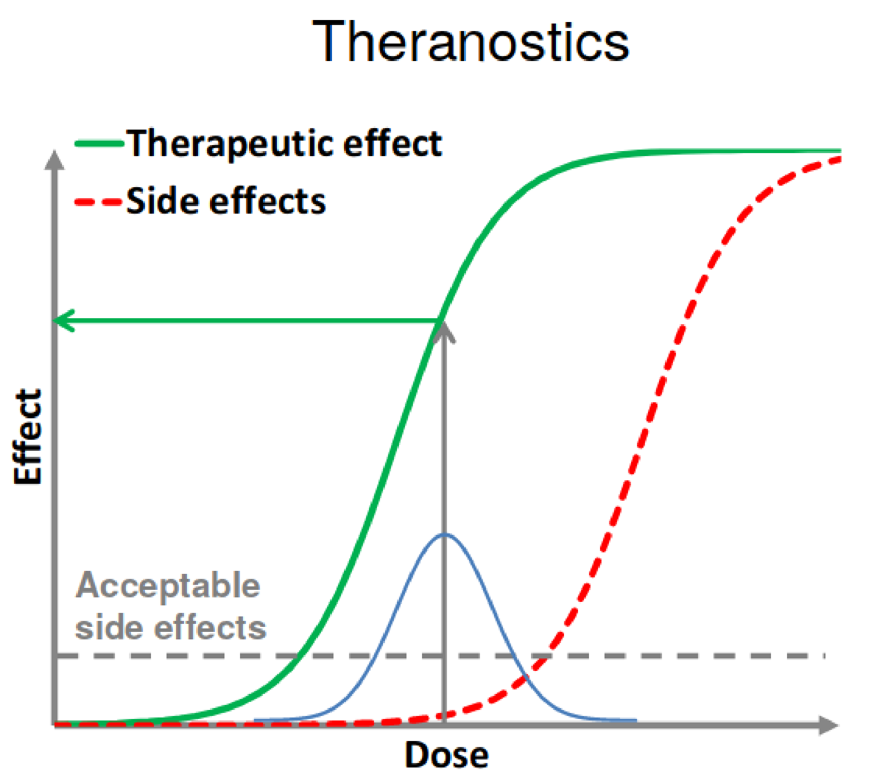

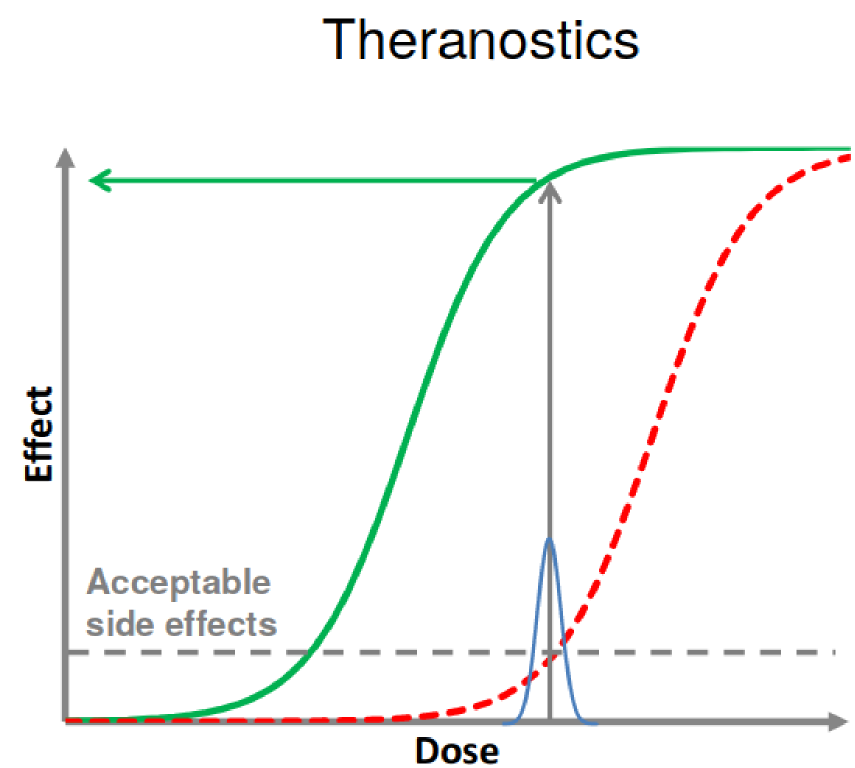

Accurate dosimetry is essential for optimum use of the therapeutic window !!!

Introduction to radiotargeted therapy

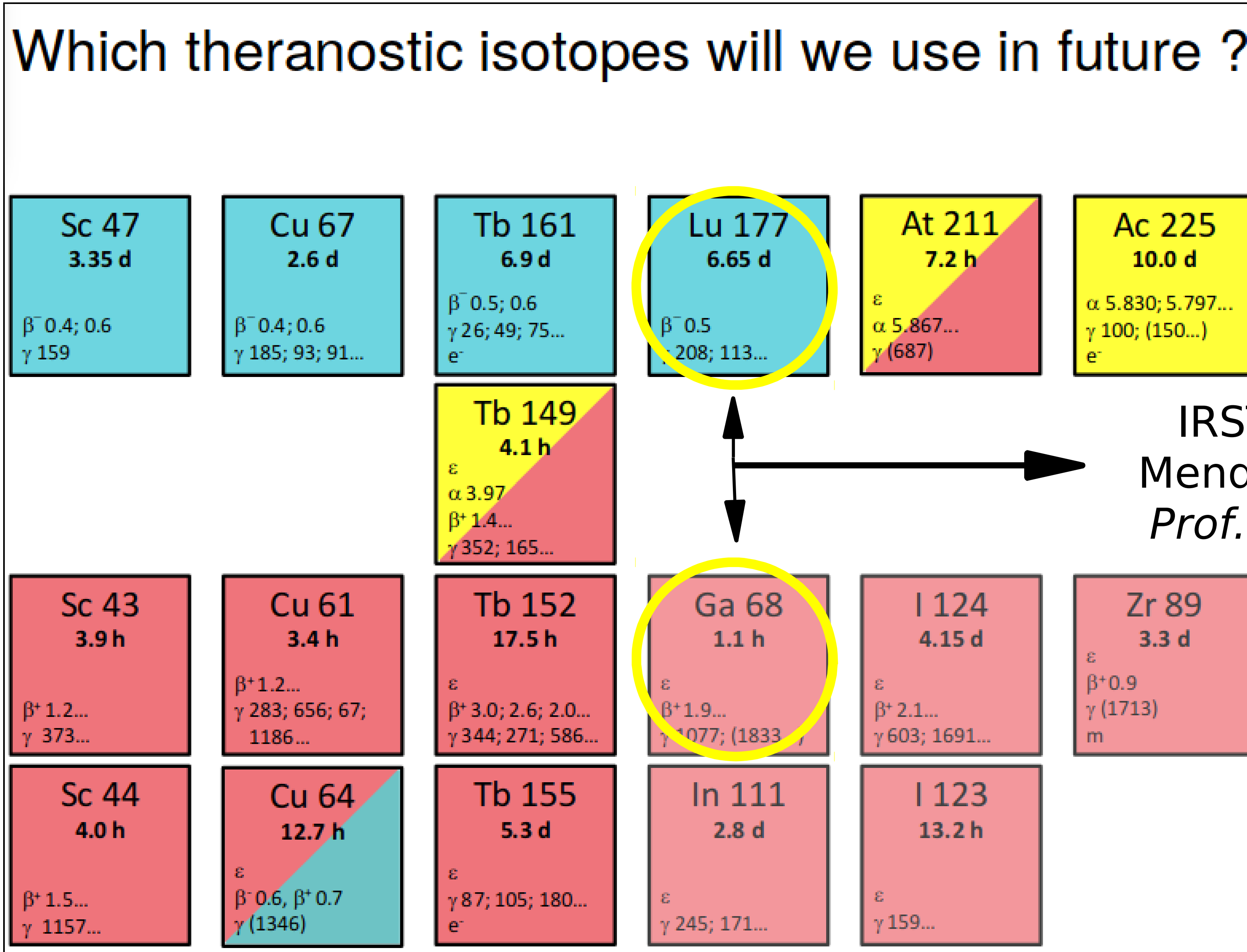

IRST IRCCS
Mendola, Italy,
Prof.Paganelli

Manifacturing radionuclides

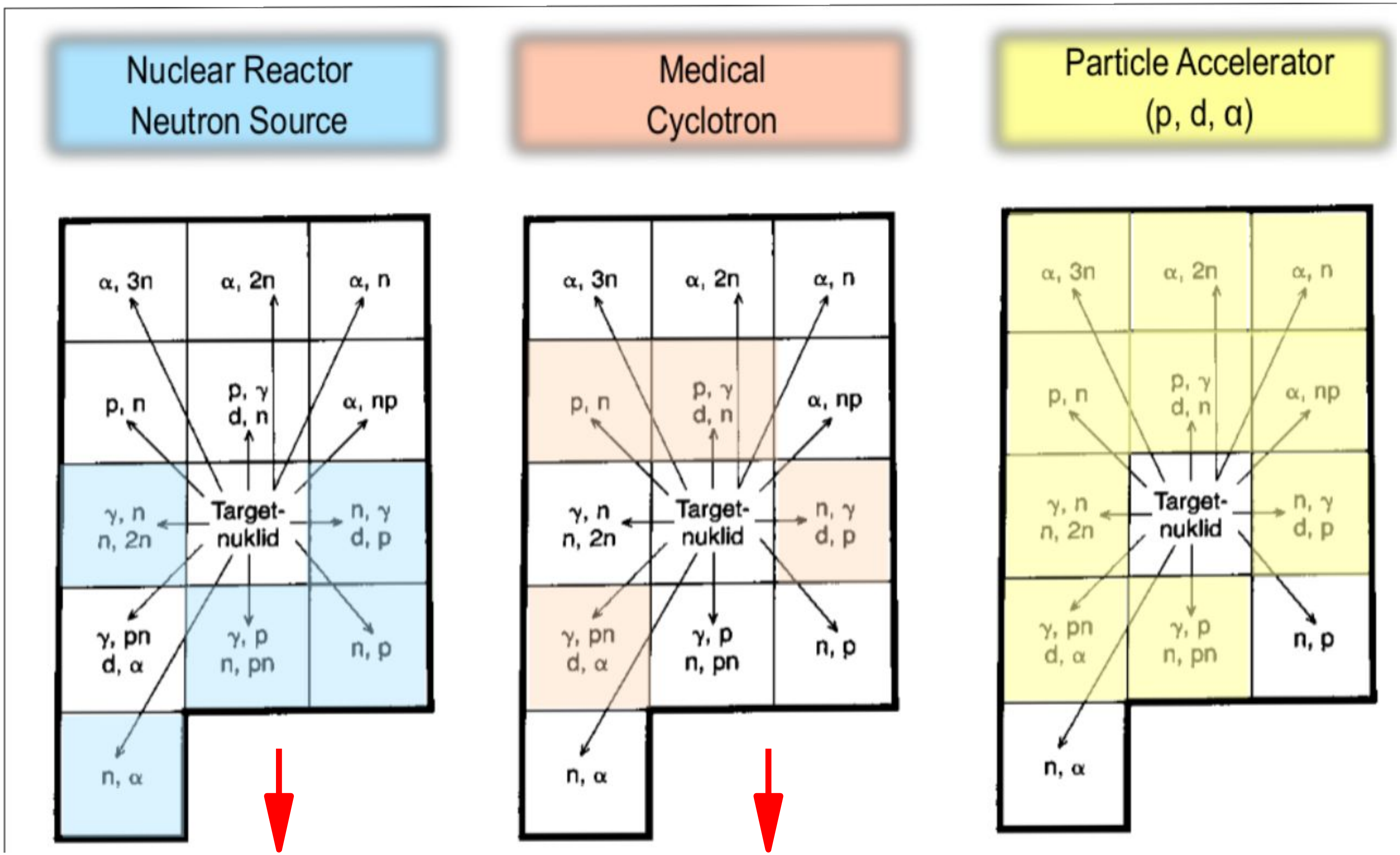

Often Beta- emitter
Therapy nuclides

Often Beta+ emitter
PET nuclides

SPES INFN – Legnaro Padova

The new 70 MeV proton cyclotron @ INFN-LNL

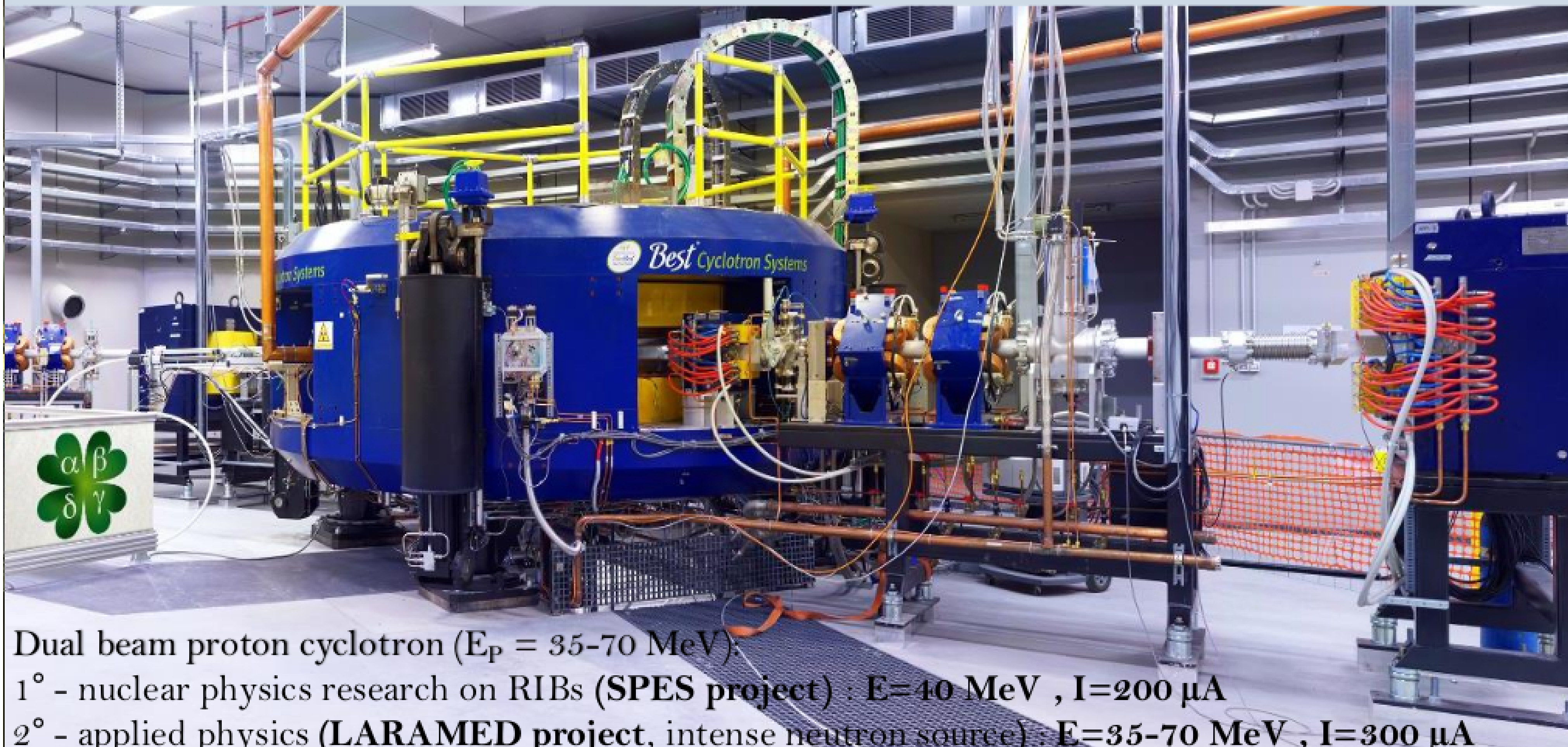

DUAL RADIO PHARMACEUTICAL PRODUCTION:
LARAMED - ISOLPHARM

Introduction to radiotargeted therapy

Four Pillars of Radionuclide Development Work

JÜLICH
FORSCHUNGSZENTRUM

Syed M Qaim,
Lecture IAEA, dec 2018

IAEA 473 technical report 2021

- Nuclear data
  - decay properties
  - production cross sections
- High current targetry
- Chemical processing
  - isolation of radionuclide and recovery of enriched target material
- Quality control
  - radionuclidic, radiochemical, chemical, specific activity

The case of ^{47}Sc

Isotope	Half-life	β^+ $E_{average}$ [KeV](I)	X and γ [KeV] (I)	β^- $E_{average}$ [KeV](I)
^{47}Sc	3.35 d	-	159.38 (68.3%)	162 (100%)
^{43}Sc	3.9 h	476 (88.1%)	372 (23%)	-
^{44}Sc	4.0 h	632 (94.27 %)	1157 (100%)	-

PET SPECT Therapy

cf. Review
Qaim, Scholten, Neumaier, JRNC **318**, 1493 (2018)

Production route	Irradiation	Batch yield	Laboratoy
^{47}Ti(n,p)^{47}Sc	Fission spectrum	1.6 GBq	Brookhaven, 1998
^{48}Ti(γ,p)^{47}Sc	40 MeV	186 MBq (3 g TiO_2 target)	Argonne, 2018
^{46}Ca(n,γ)^{47}Ca $\xrightarrow{\beta^-}$ ^{47}Sc	High thermal neutron flux	600 MBq 1 mg target, ^{46}Ca (31.7 % enriched)	Grenoble/PSI, 2014
^{48}Ti(p,2p)^{47}Sc	48 < 150 MeV	900 MBq Purity not acceptable	Brookhaven, 1998
^{48}Ca(p,2n)^{47}Sc	24 → 17 MeV	~ 10 MBq	Warsaw, 2017

All methods of ^{47}Sc production need further development.

Isotope	half-life
^{43}Sc	3.89 h
^{44g}Sc	3.97 h
^{44m}Sc	58.6 h
^{45}Sc	stable
^{46g}Sc	83.79 d
^{46m}Sc	18.75 s
^{47}Sc	3.35 d
^{48}Sc	43.67 h
^{49}Sc	57.2 m

The case of ^{47}Sc

Enriched materials are VERY expensive!

Target (abundance)	Measured cross section	Comment
Ti-48 (73.73%)	• *Gadioli et al* (1981): **Sc-47**, Sc-46, Sc-44, Sc-43 (V-48, V-47, K-43, K-42, Cl-39, Cl-34m) ▪ *Levkovskij* (1991): **Sc-47**, Sc-44m, Sc-44 (V-48, V-47)	Experiments done with oxide Ti-48 (99.1%) Not all the contaminant radionuclides were measured → **It is important to verify the cross sections** by using updated nuclear data and metal targets (highest available enrichment)
Ti-49 (5.41%)	▪ *Levkovskij* (1991): Sc-48, Sc-46 (V-48)	**No experimental data available for Sc-47**
Ti-50 (5.18%)	• *Gadioli et al* (1981): Sc-48, **Sc-47**, Sc-46, Sc-44, Sc-43 (K-43, K-42, Cl-39, Cl-38)	Experiments done with oxide Ti-50 enriched 69.7% and corrected with exp data for contamination of Ti-48 (23%) and theoretical data for Ti-49 (2.0%), Ti-47 (2.4%) and Ti-46 (3.1%)
V-nat (V-51: 99.750%)	➢ **Many authors**: Sc-48, **Sc-47**, Sc-46, Sc-44m, Sc-44, Sc-43 (V-48, Cr-48, Cr-49, Cr-51, K-43, K-42)	Very interesting due to the **low cost** and **highly available material**; it is important to **verify quantity and quality of produced Sc-47**

Nuclear reaction calculations ...

TIME SCALES AND ASSOCIATED MODELS

62 MeV ^{56}Fe (p,xp)
Double differential cross sections

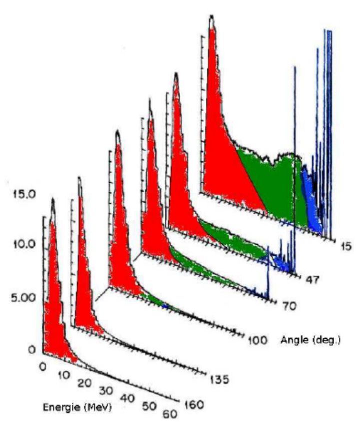

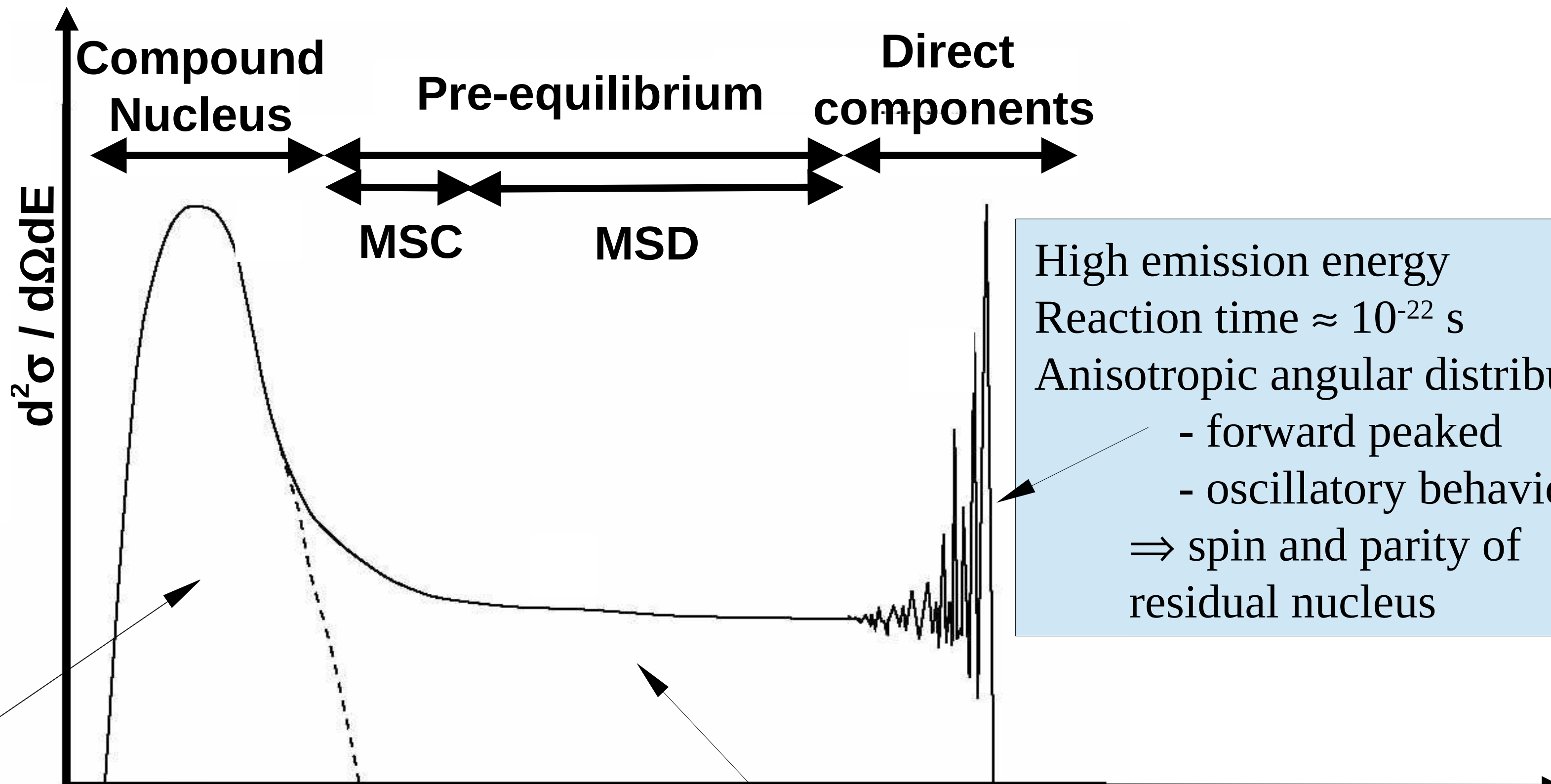

High emission energy
Reaction time ≈ 10^{-22} s
Anisotropic angular distribution
- forward peaked
- oscillatory behavior

⇒ spin and parity of residual nucleus

Low emission energy
Reaction time ≈ 10^{-18} s
Isotropic angular distribution

Intermediate emission energy
Intermediate reaction time
Anisotropic angular distribution smoothly increasing to forward peaked shape with outgoing energy

Emission energy

Reaction time

Nuclear reaction theory: general

S-matrix: the response of the target

The S-matrix measures the response of the target: a real potential cannot create or destroy particles, it can change only the phase of the outgoing wave, not the modulus

$$S_\ell = e^{2i\delta_\ell}$$

The total elastic cross section becomes:

$$\sigma_{el} = \frac{\pi}{k^2}\sum_{0}^{\infty}(2\ell+1)|S_\ell - 1|^2$$

No nuclear reactions here!

Nuclear reaction theory: general

loss of elastic flux: $|S_\ell| < 1$

$$\sigma_{el} = \frac{\pi}{k^2}\sum_0^\infty (2\ell+1)|S_\ell - 1|^2$$

$$\sigma_r = \frac{\pi}{k^2}\sum_0^\infty (2\ell+1)(1-|S_\ell|^2)$$

$$\sigma_{tot} = \sigma_{el} + \sigma_r = \frac{\pi}{k^2}\sum_0^\infty (2\ell+1)(1-\mathcal{R}eS_\ell)$$

The transmission coefficient T_ℓ is

$$T_\ell = 1 - |S_\ell|^2 \qquad (5)$$

Nuclear reaction theory: general

Optical Potential U(r)

Coulomb part: $V_C(r) = Z_1 Z_2 e^2/r$

Real Nuclear part: $V(r)$ for nuclear attraction

Imaginary Part $W(r)$: for reaction to occur

Spin-Orbit part: $V_{SO}(r)$ Important ingredient of nuclear force and for polarization data

$$U(r) = V_C(r) + V(r) + iW(r) + V_{SO}(r)$$

Nuclear reaction theory: compound

CN basics

1. Continuum overlapping levels
2. Independence initial/exit channel

$$\sigma_{ab} = \sigma_a^{CN} P_b$$

Hauser-Feshbach formula:

$$\sigma_{ab} = \frac{\pi\, T_a}{k_a^2} \frac{T_b}{\sum_c T_c}$$

Need transmission coefficients (from optical potentials)

Nuclear reaction theory: Compound

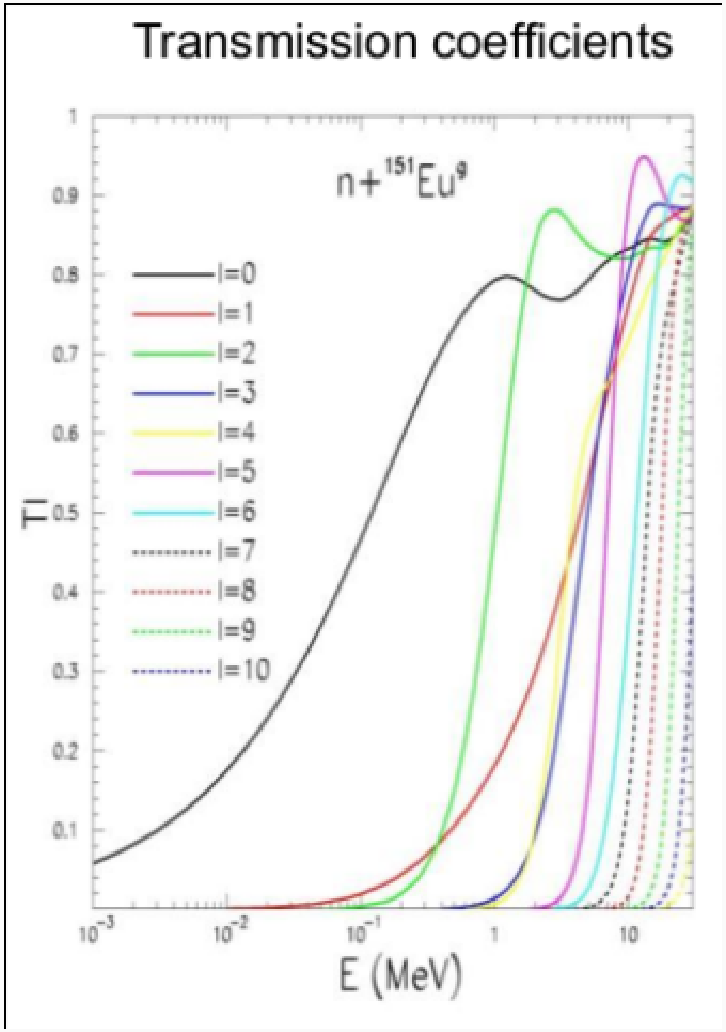

Nuclear reaction theory: Compound

CN Basic 2, complexities

Loop over angular momentum and parity

$$\sigma_{ab} = \frac{\pi}{k_a^2} \sum_{J,\pi} \sum_{\alpha,\beta} \frac{2J+1}{(2s+1)(2I+1)} \frac{T_a^{J,\pi}(\alpha) T_b^{J,\pi}(\beta)}{\sum_\delta T_d^{J,\pi}(\delta)}$$

Adding the WIDTH-FLUCTUATION CORRECTION

$$\sigma_{ab} = \frac{\pi}{k_a^2} \sum_{J,\pi} \sum_{\alpha,\beta} \frac{2J+1}{(2s+1)(2I+1)} \frac{T_a^{J,\pi}(\alpha) T_b^{J,\pi}(\beta)}{\sum_\delta T_d^{J,\pi}(\delta)} \mathbf{W}_{\alpha,\beta}$$

Adding the DENSITY OF RESIDUAL NUCLEUS LEVELS

$$\sigma_{ab} = \frac{\pi}{k_a^2} \sum_{J,\pi} \sum_{\alpha,\beta} \frac{2J+1}{(2s+1)(2I+1)} \frac{T_a^{J,\pi}(\alpha) < \mathbf{T}_\mathbf{b}^{\mathbf{J},\pi}(\beta) >}{\sum_\delta < \mathbf{T}_\mathbf{d}^{\mathbf{J},\pi}(\delta) >} W_{\alpha,\beta}$$

Nuclear reaction theory: compound

Averaging over Residual Nucleus Density Levels

Emission $\rightarrow$ discrete level with energy E_b

$$< T_b(\beta) >= T_b^{J\pi}(\beta) \text{ (from O.M.Potential)}$$

Emission in the continuum level

$$< T_b(\beta) >= \int_E^{E+\Delta E} T_b^{J\pi}(\beta)\rho(E, J, \pi)dE$$

$\rho(E, J, \pi)$ DENSITY of residual nuclear levels (J, π) with excitation energy E

Nuclear reaction theory: compound

CN multiple emissions

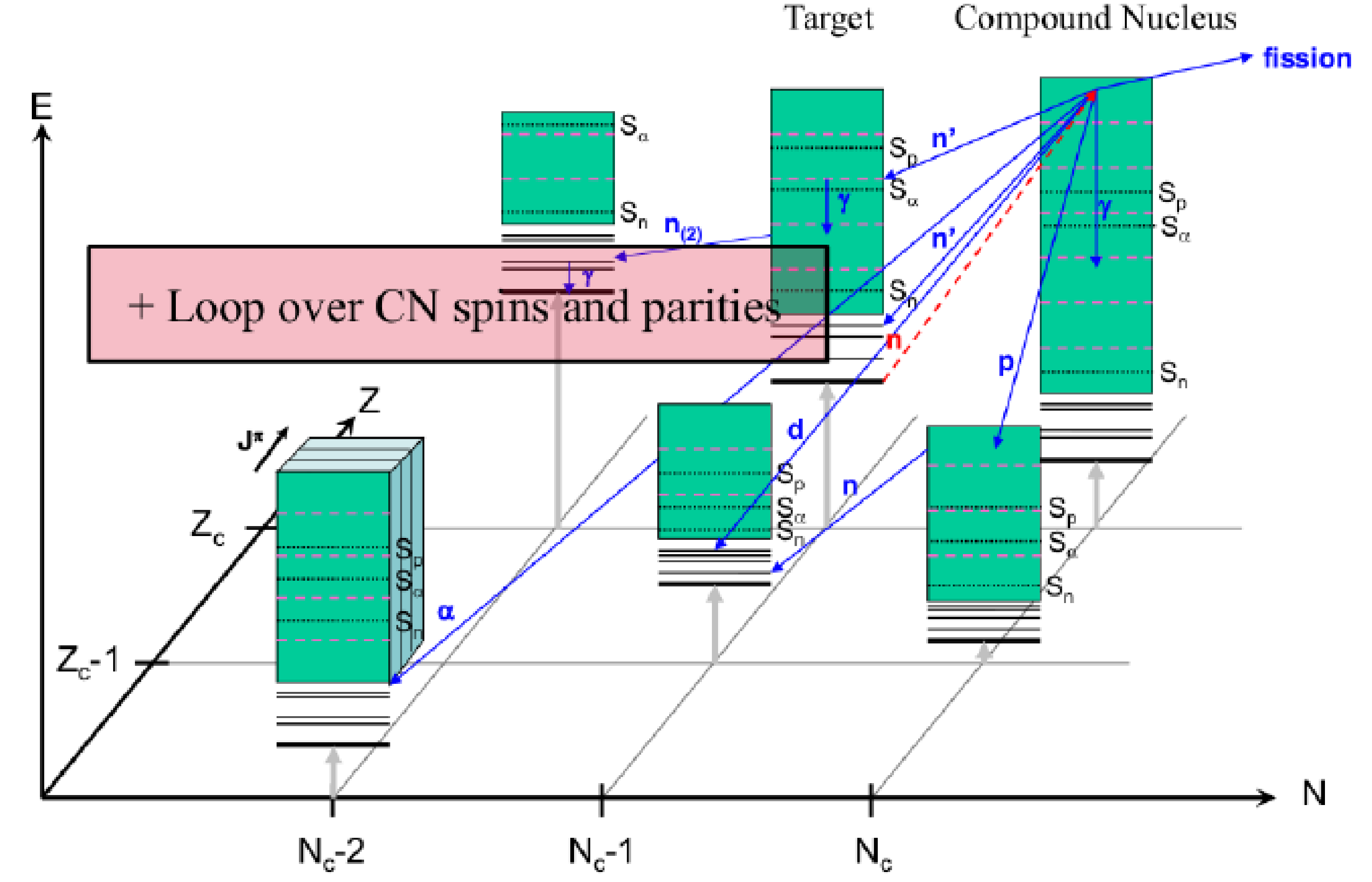

Nuclear reaction theory: compound

Level Density : overview

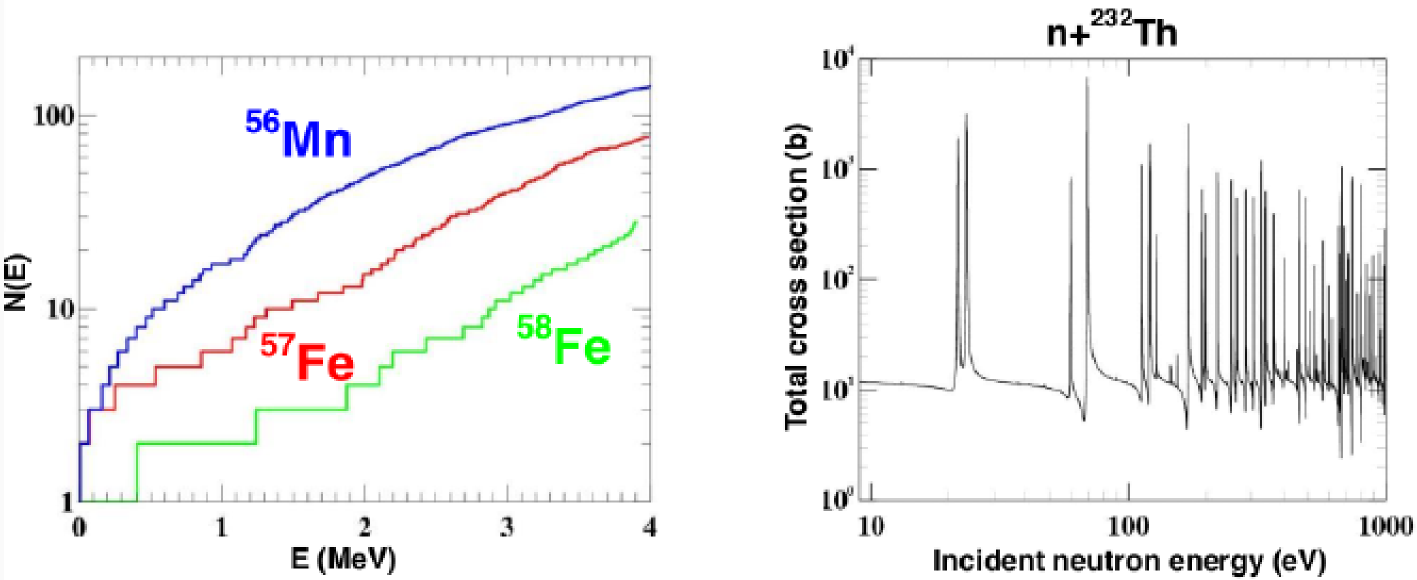

- Exponential increase of the cumulated number of discrete levels N(E) with energy
- $\Rightarrow \rho(E) = \frac{dN(E)}{dE}$ increases exponentially

$\Rightarrow$ odd-even effects

Nuclear reaction theory: compound

Level Density : general description

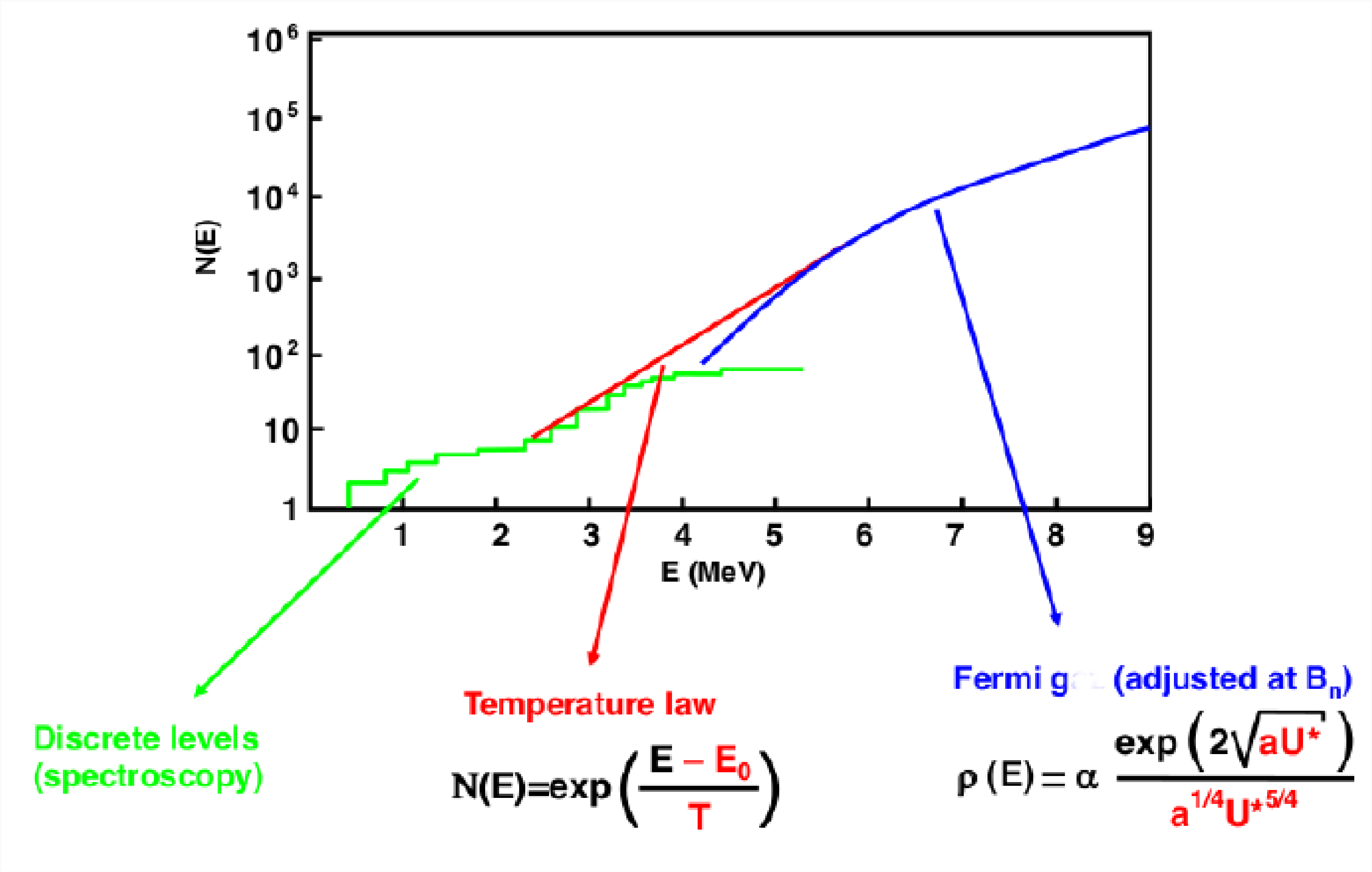

Nuclear reaction theory: pre-equilibrium

Angular/energy distributions

62 MeV ^{56}Fe (p,xp)
Double differential cross sections

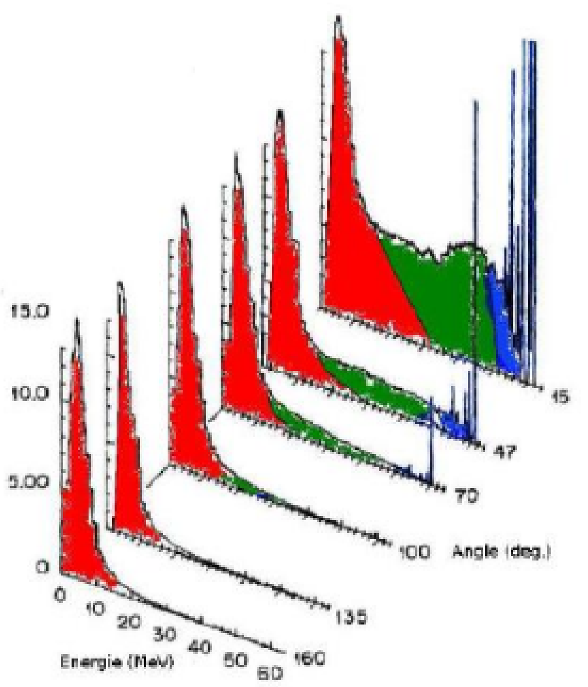

- Always evaporation peak
- Discrete peaks at forward angles
- **Flat intermediate region**

Nuclear reaction theory: pre-equilibrium

Sketch of the excitation model

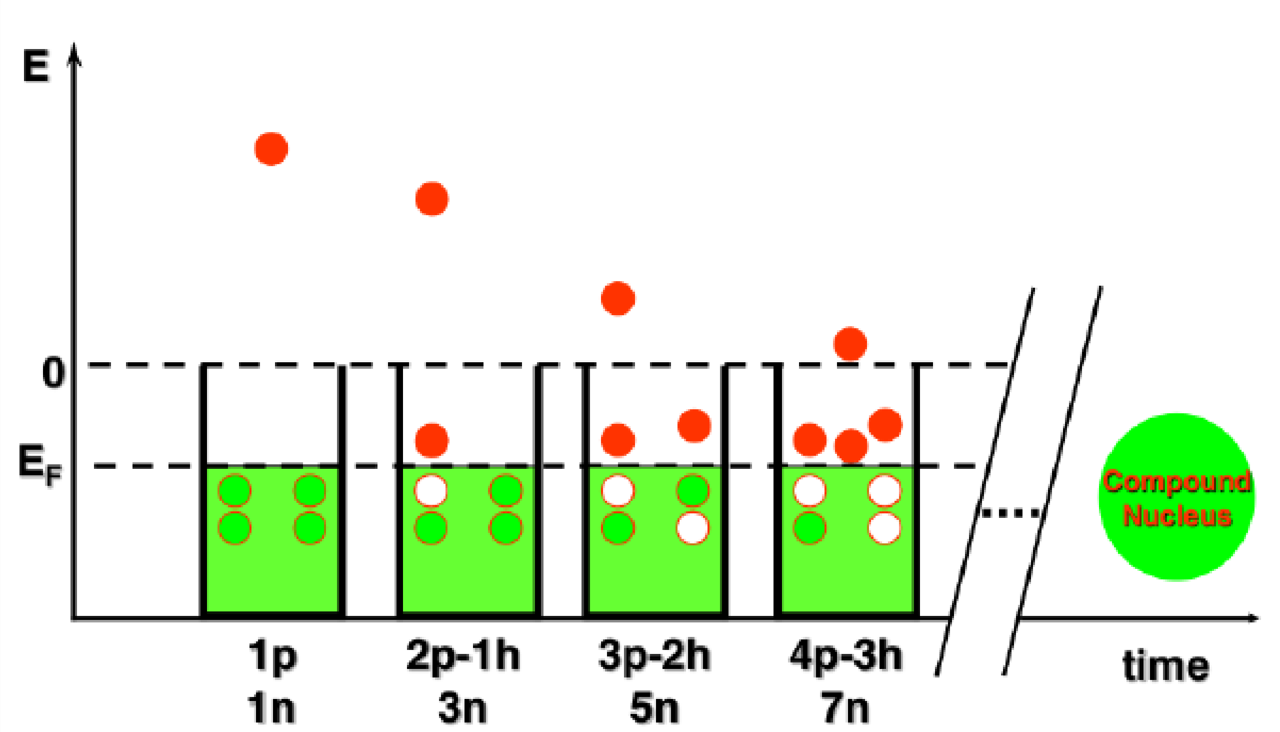

Nuclear reaction theory: pre-equilibrium

Sketch of the master equation

– $q(n,E,t)$ Probability of finding the composite system in exciton n and energy E
– $\lambda^{\pm}(n,E)$ Transition rate $n \to n \pm 2$
– $w(n,E)$ Total emission rate from n excitons

$$\begin{aligned}\dot{q}(n,t) &= \lambda^{+}(n-2)q(n-2,t) + \lambda^{-}(n+2)q(n+2,t) \\ &\quad -(\lambda^{+}(n) + \lambda^{-}(n) + w(n))q(n,t)\end{aligned}$$

$$\frac{d\sigma^{P.E.}}{dE}(a,b) = \sigma_a \sum_{n,\Delta n=2} w_b(n,E) \int_0^{\infty} q(n,E,t)dt$$

Nuclear reaction calculations … codes

Talys 1.9, Fluka dev 2018.1, Empire 3.2

A. Koning, et al."TALYS: A nuclear reaction program", User Manual (2015)

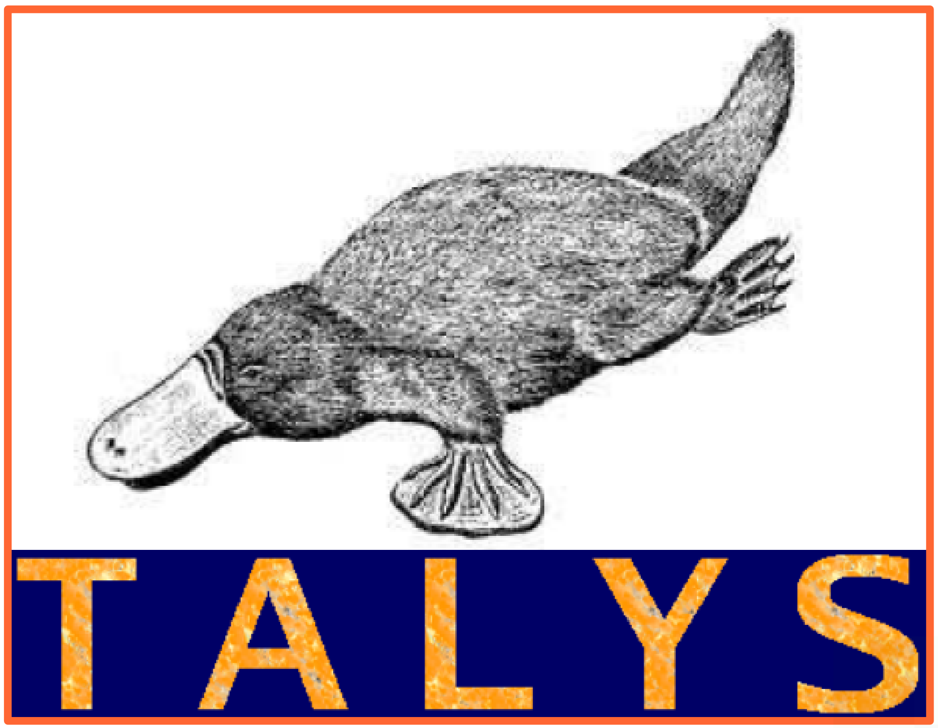

(developed by NRG–CEA)

EMPIRE

Nuclear Reaction Model Code

M. Herman, et al, "EMPIRE: Nuclear Reaction Model Code System for Data Evaluation", Nucl. Data Sheets, 108 (2007) 2655-2715.

(maintained by IAEA)

T.T. Böhlen, et al."The FLUKA Code: Developments and Challenges for High Energy and Medical Applications", Nuclear Data Sheets 120, 211-214 (2014)

(developed by INFN-CERN)

FLUKA

Nuclear Reaction Calculations

Table 1: Pre-equilibrium (PE) and level density (LD) Models used by the referenced codes. [1]

Code	Pre-equilibrium Model		Level density Model	
Talys	1	Exciton (analytical)	1	CT+FG
	2	Exciton (numerical)	2	BSFG
	3	Exciton + Optical	3	GSFM
	4	MSD/MSC	4	Microscopic (Goriely)
	(5)	New Exciton Geometry dependent	5	Microscopic (Hilaire)
			6	T-dep HFB
Empire	HMS		EGSM	
Fluka	PEANUT		Modified FG	

[1] MSD: Multi-Step Direct, MSC: Multi-Step Compound, CT: Constant temperature, FG: Fermi Gas, BSFG: Back Shifted Fermi Gas, GSFM: Generalized SuperFluid Model, HFB: Hartree-Fock-Bogliubov. PEANUT: Pre-equilibrium Approach to NUclear Thermalization, HMS: Hybrid Montecarlo Simulation, EGSM: Enhanced Generalized Superfluid Model.

The importance of RIPL

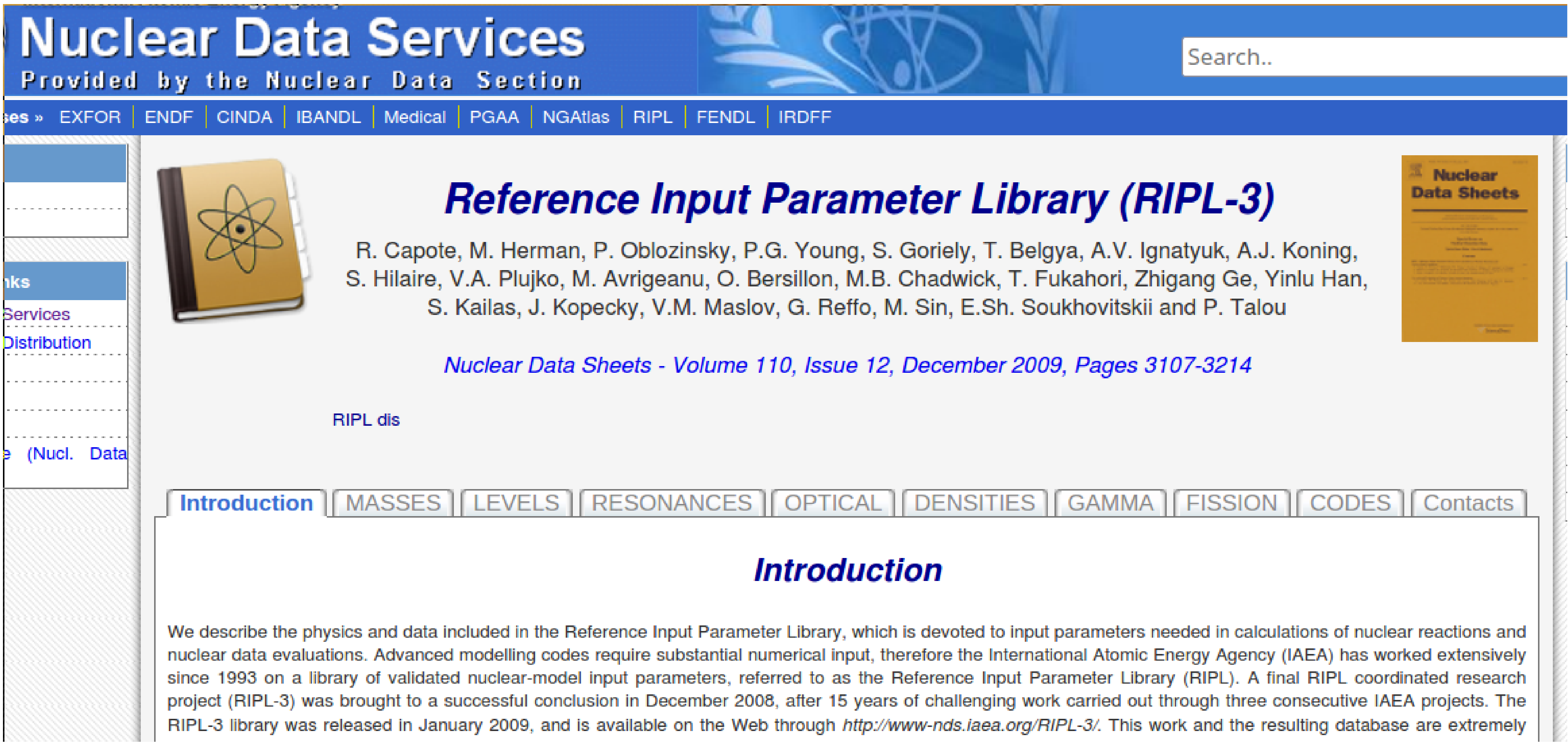

Nuclear Data Services

Provided by the Nuclear Data Section

Search..

ses » EXFOR | ENDF | CINDA | IBANDL | Medical | PGAA | NGAtlas | RIPL | FENDL | IRDFF

nks

Services

Distribution

e (Nucl. Data

Reference Input Parameter Library (RIPL-3)

R. Capote, M. Herman, P. Oblozinsky, P.G. Young, S. Goriely, T. Belgya, A.V. Ignatyuk, A.J. Koning, S. Hilaire, V.A. Plujko, M. Avrigeanu, O. Bersillon, M.B. Chadwick, T. Fukahori, Zhigang Ge, Yinlu Han, S. Kailas, J. Kopecky, V.M. Maslov, G. Reffo, M. Sin, E.Sh. Soukhovitskii and P. Talou

Nuclear Data Sheets - Volume 110, Issue 12, December 2009, Pages 3107-3214

Nuclear Data Sheets

RIPL dis

Introduction | MASSES | LEVELS | RESONANCES | OPTICAL | DENSITIES | GAMMA | FISSION | CODES | Contacts

Introduction

We describe the physics and data included in the Reference Input Parameter Library, which is devoted to input parameters needed in calculations of nuclear reactions and nuclear data evaluations. Advanced modelling codes require substantial numerical input, therefore the International Atomic Energy Agency (IAEA) has worked extensively since 1993 on a library of validated nuclear-model input parameters, referred to as the Reference Input Parameter Library (RIPL). A final RIPL coordinated research project (RIPL-3) was brought to a successful conclusion in December 2008, after 15 years of challenging work carried out through three consecutive IAEA projects. The RIPL-3 library was released in January 2009, and is available on the Web through *http://www-nds.iaea.org/RIPL-3/*. This work and the resulting database are extremely

Modeling of the relevant **cross sections** with nuclear reaction code

TALYS

1 – 4 **pre-equilibrium** models
1 – 6 **level density** models

24 combinations of models
(or 30 with pre-equilibrium 5)

Talys default
& adjusted

Statistical band & **BTE**

$$BTE = \frac{Q_1 + Q_3}{2}$$

Talys modified

c normalization
p energy shift

$$\rho(E) = \exp\left(c\sqrt{E-p}\right)\rho(E-p)$$

Phys.Rev.C 104 (2021) 4, 044619

^{50}Ti – statistical band & BTE

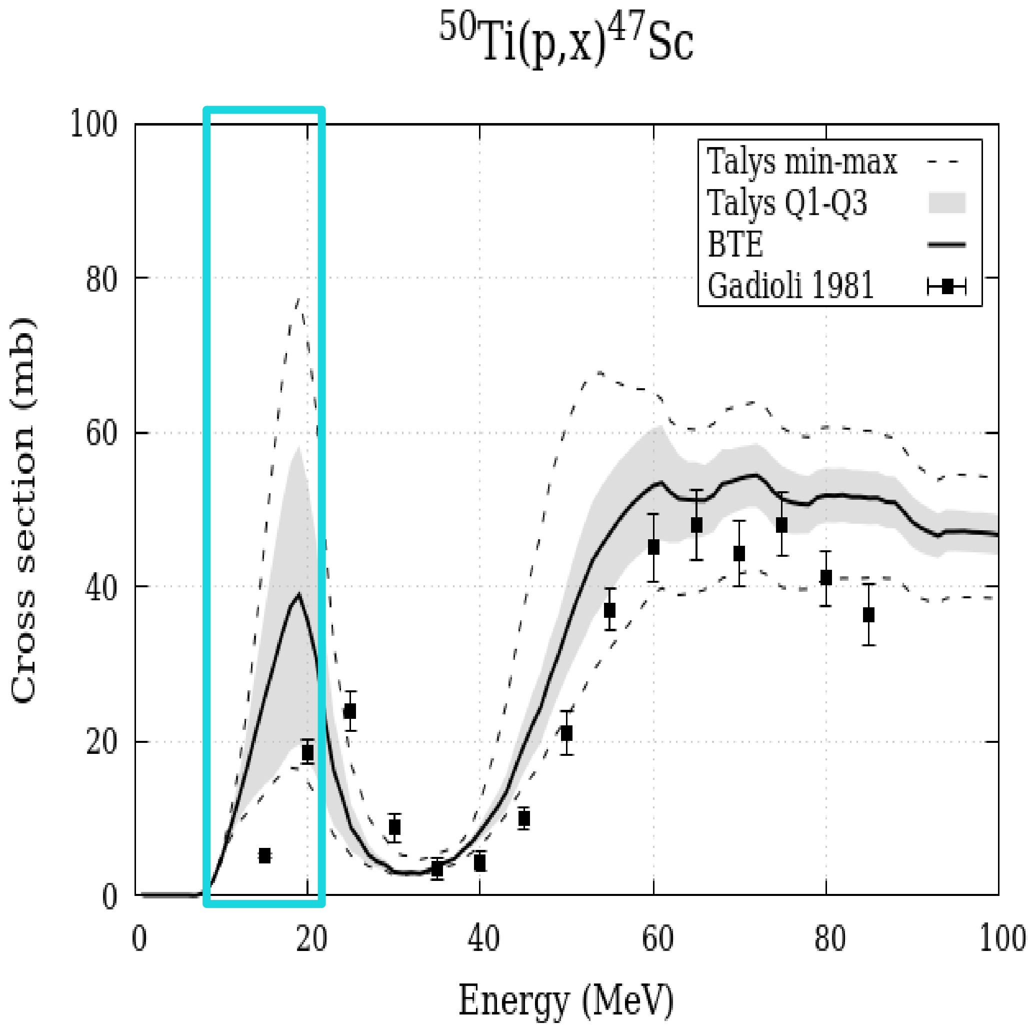

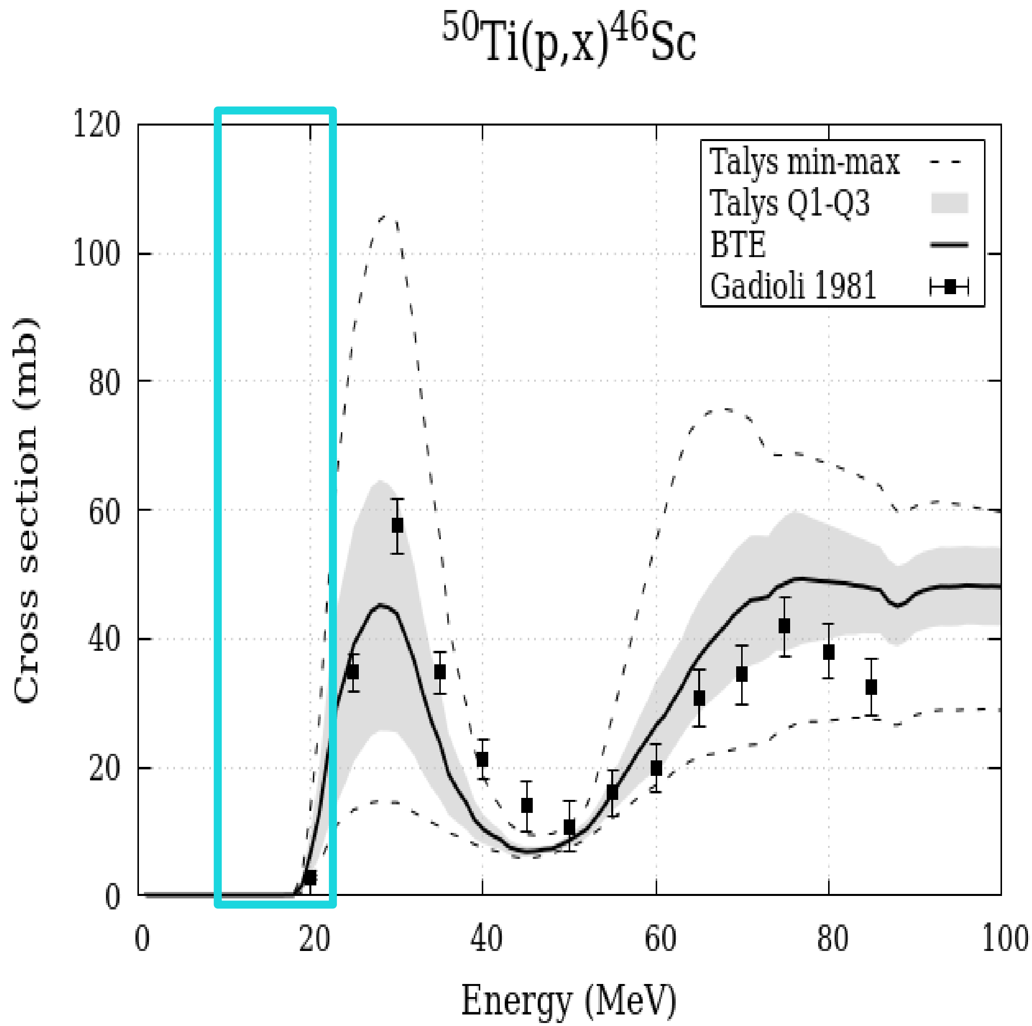

^{49}Ti – statistical band & BTE

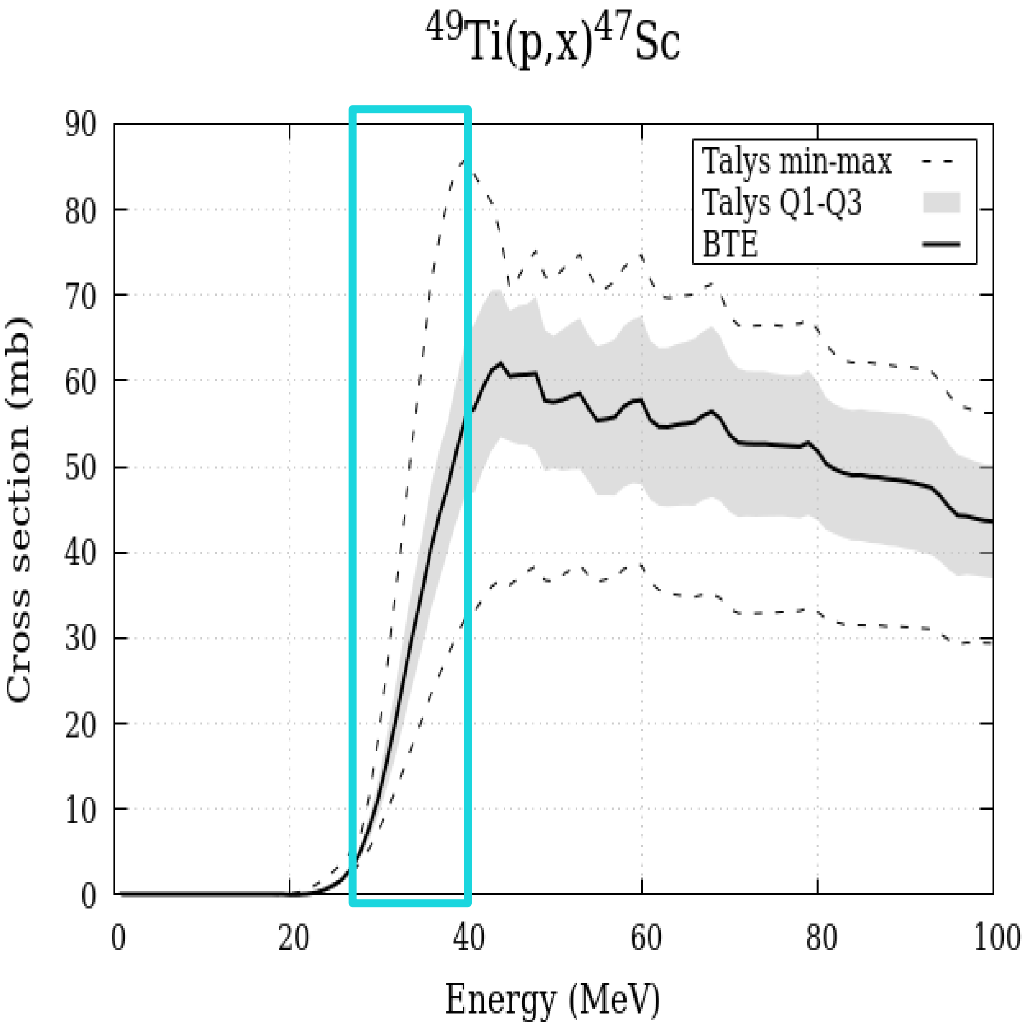

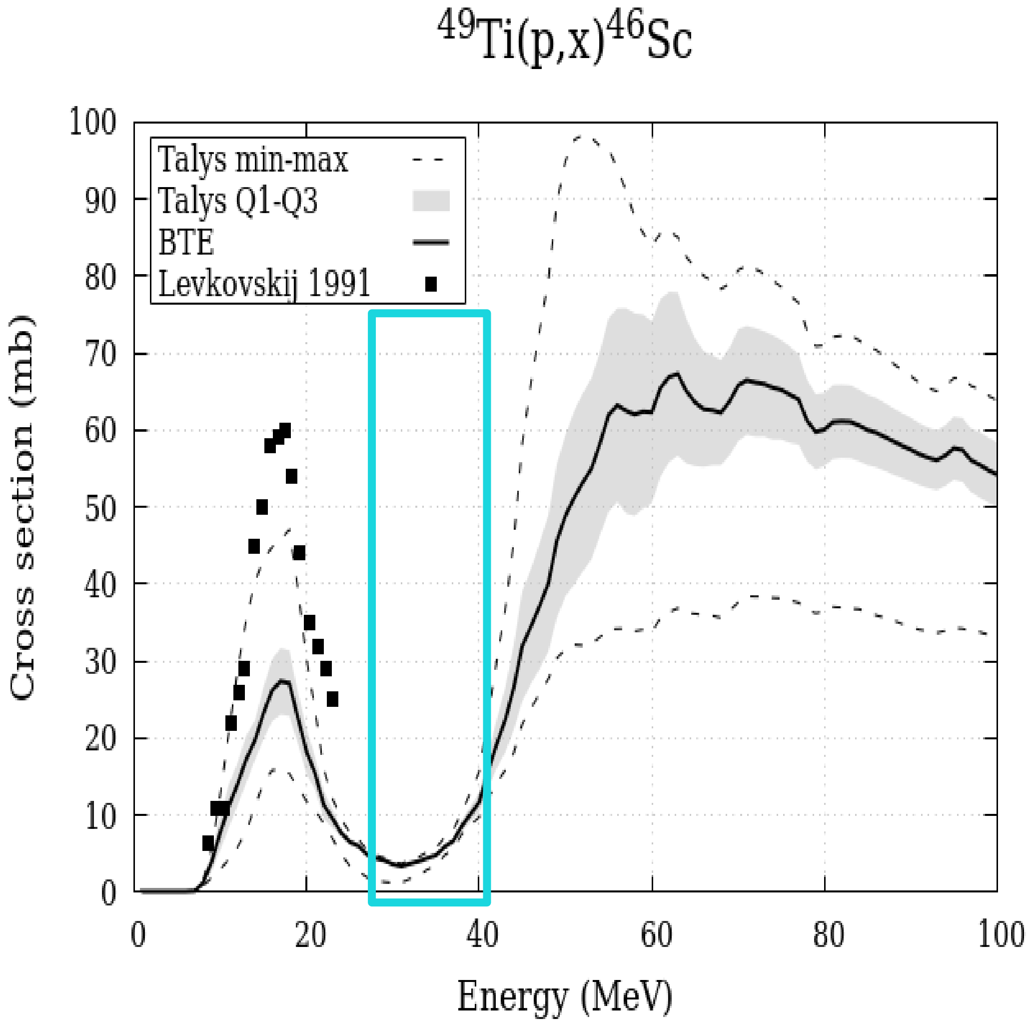

Microscopic NLD parameter optimization

NEW DATA FROM REMIX! WORLD FIRST MEASUREMENT OF SC47 PRODUCTION FROM ENRICHED TI47 TARGETS…...

PE 5 → Geometry Dependent Hybrid (GDH) model

LD 4 → Microscopic Hartree-Fock Nuclear Level Densities

(Skyrme Force, Goriely's tables)

$$\rho(E) = \exp\left(c\sqrt{E-p}\right)\rho(E-p)$$

OPTIMIZATION

Based on **Genetic Algorithms**
Multiparameter optimization for all related measured cross sections Sc(43,44g,44m,46,47,48); K(42,43); V(48)

Genetic Algorithms

Genetic Algorithm: optimization inspired by Darwin's theory of natural evolution.

Codifica del problema in "cromosomi"

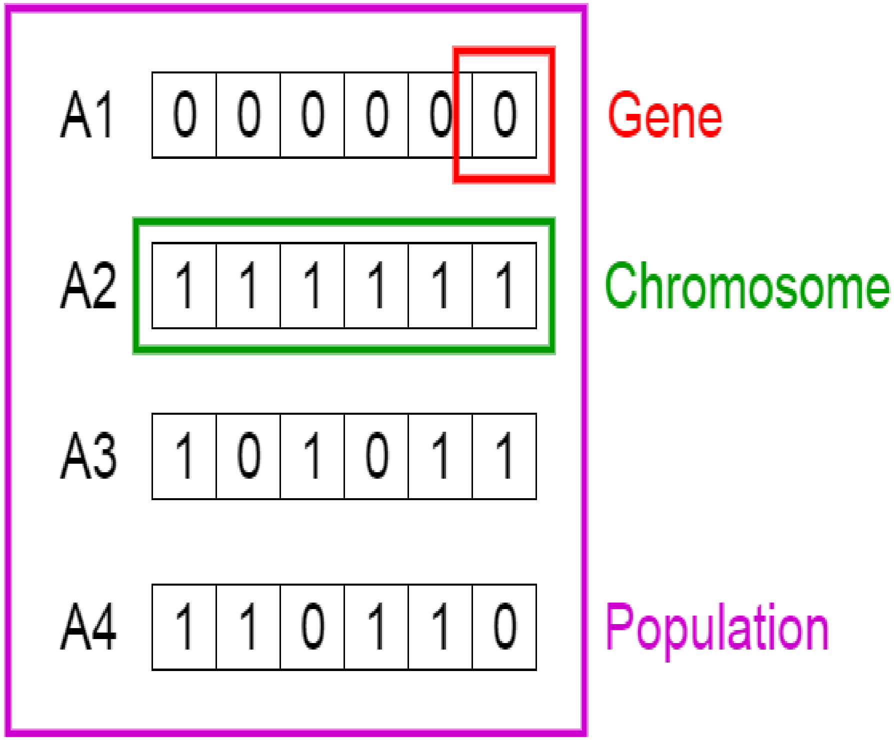


```
START
Generate the initial population
Compute fitness
REPEAT
    Selection
    Crossover
    Mutation
    Compute fitness
UNTIL population has converged
STOP
```

^{49}Ti – Genetic Algoritm for NLD

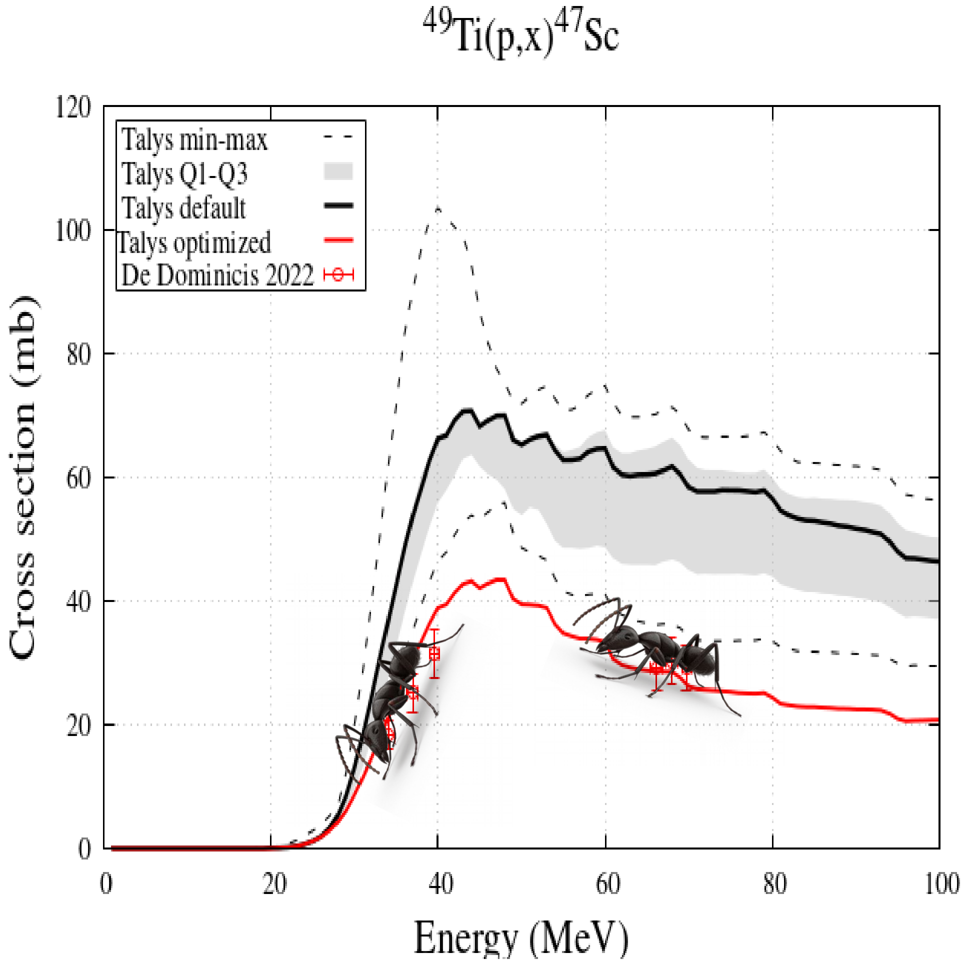

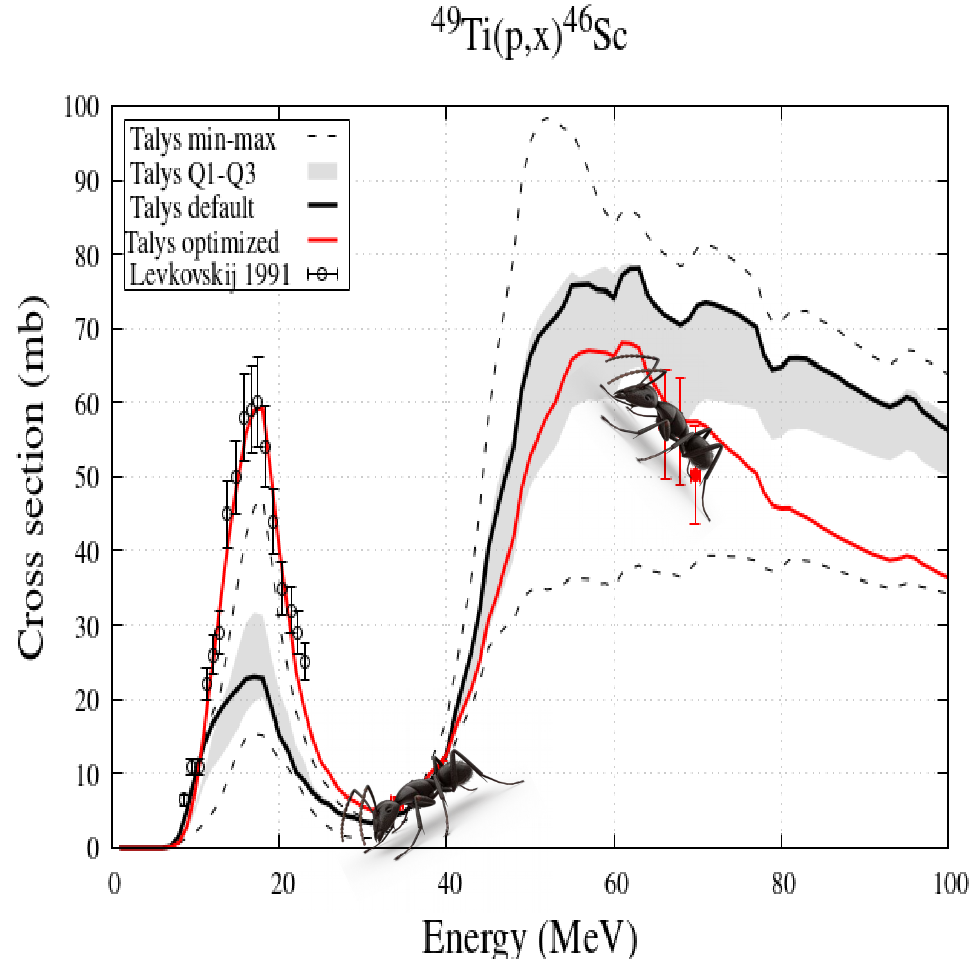

Preliminary REMIX data not yet validated and not public.

Previous experience with Vnat targets Phys Rev C 2021

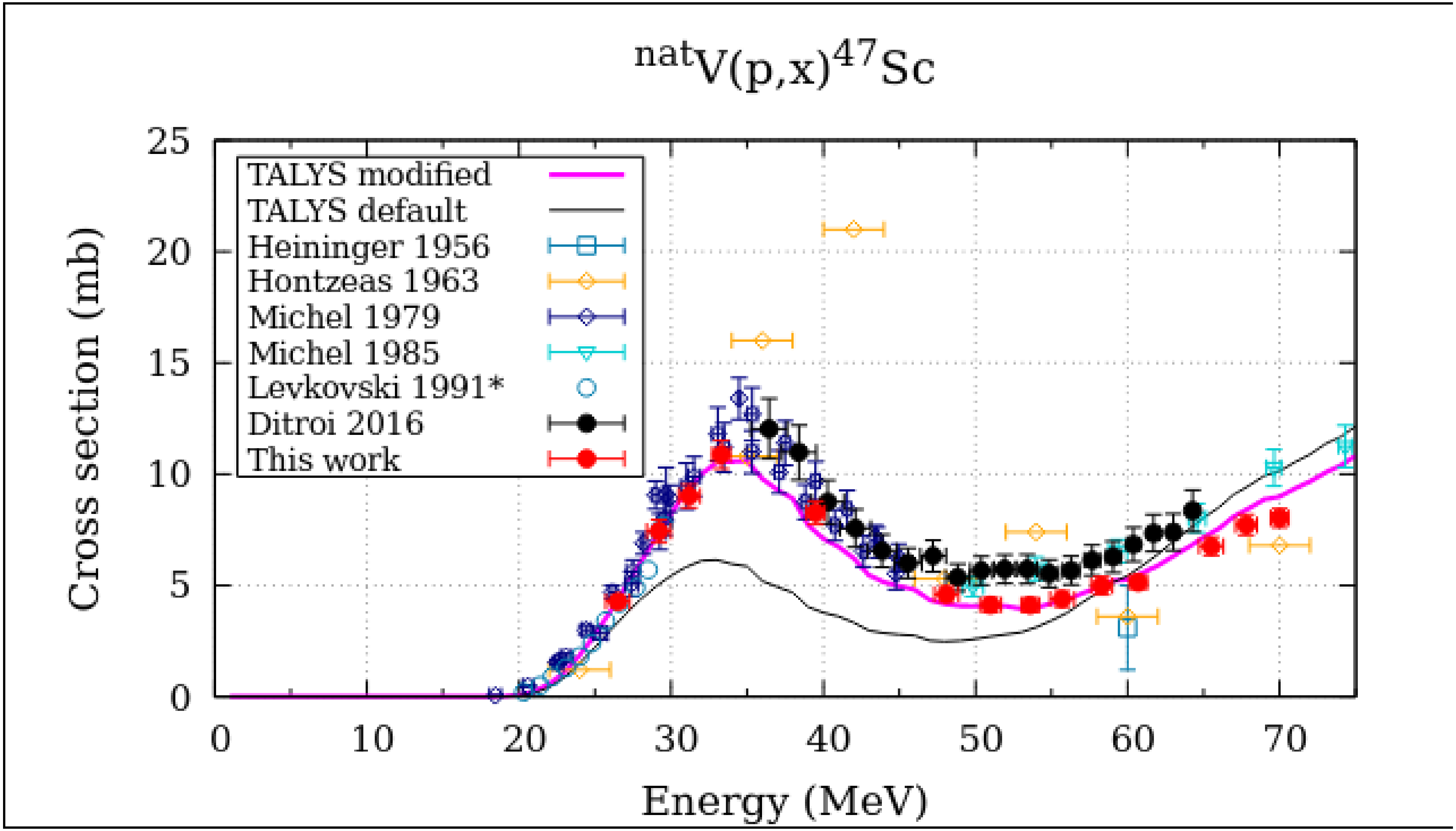

Path to assess the production route

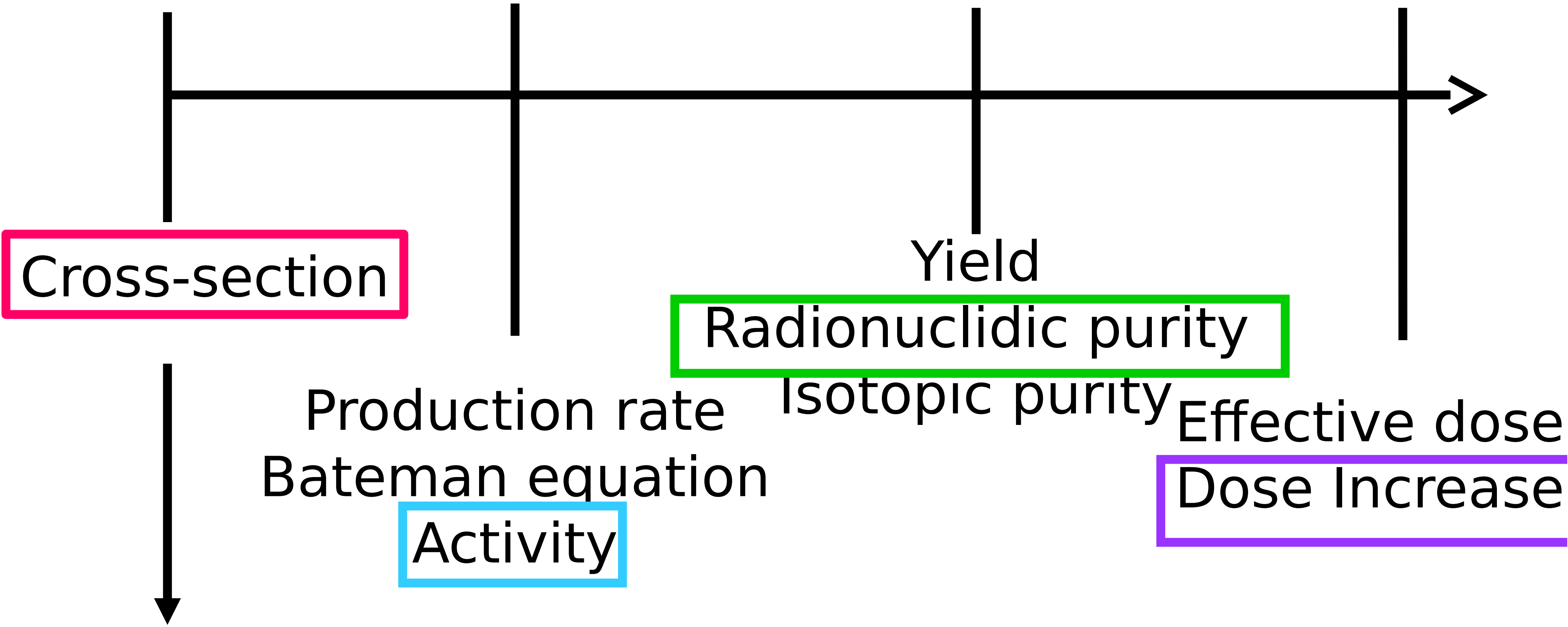

nuclear reaction

codes supported by nuclear data

Path to assess the production route (depends on irradiation conditions)

European Pharmacopoeia requires a radionuclidic purity (RNP) greater than **99%**

$$RNP = \frac{A_{52gMn}}{\sum_i A_i}$$

^{52g}Mn case

Dose Increase (DI) caused by the impurities should be maintained within the **10% limit**

$$\boldsymbol{DI} = \frac{ED_t(t)}{ED_{52gMn}}$$

^{52g}Mn case

Path to assess the 2 production routes (^{52g}Mn case)

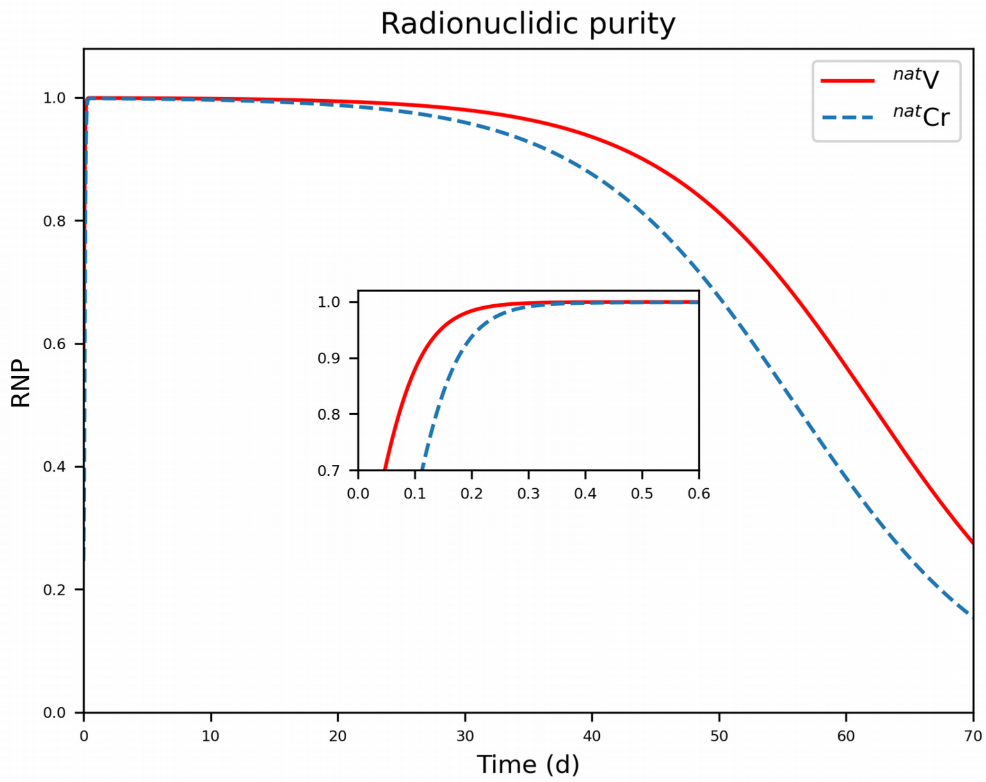

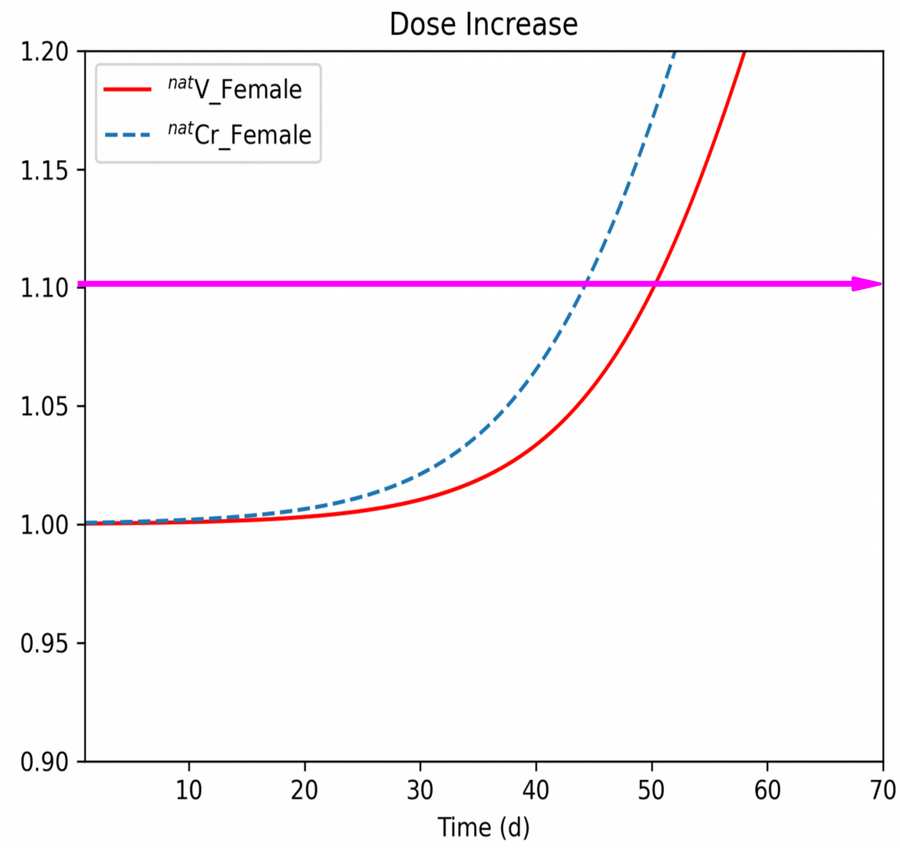

Conclusion: Nucl Tecn (2022) and arXiv:2204.00402
natV(alpha,x)52gMn is more efficient than natCr(p,x)52gMn

Conclusions

- Radiopharmaceutical production is a very interdisciplinary project involving Nuclear Science and Nuclear Data for medical applications.
- Nuclear modeling (cross sections, rates, activities, purities, etc) is an important aspect together with nuclear experiments and technology.
- So far, we have assessed and compared production routes including analysis of co-produced contaminants.
- ^{47}Sc: $^{nat}V(p,x)$, $^{50}Ti(p,x)$, $^{49}Ti(p,x)$ [?]. Moderate production feasible.
- ^{52g}Mn: $^{nat}Cr(p,x)$, $^{nat}V(alpha,x)$: better V targets than Cr.
- ^{117m}Sn: $^{nat}Cd(alpha,x)$, $^{nat}In(alpha,x)$: better In than Cd.
- Next ^{155}Tb : potentially producible with hospital cyclotrons $^{155}Gd(p,n)$
- Societal impact:

  this type of research could lead to new lifesaving methods in the future.

For 1h irradiation

Target	Energy Range	47Sc (MBq/µA)	46Sc (MBq/µA)
50Ti	~ 10-20	~ 5	1.1E-4
natV	~ 20-30	~ 1.0 - 1.5	6.0E-4
49Ti	~ 30-40	~ 20	0.13

NO

Per il momento escluso, a causa della produzione del contaminante secondario 48-Sc, e non solo...

Multimodal pET/mRi Imaging with Cyclotron-produced $^{52/51}Mn$ and stable paramagnetic Mn iSotopes

PET and MRI fusion

A breakthrough in **Multi-Modal Imaging** (MMI) diagnostic procedures may be achieved with a genuine fusion between PET/SPECT and MRI analyses. However that could be obtained only by using both a radioactive and contrast agent based upon the same chemical compound.

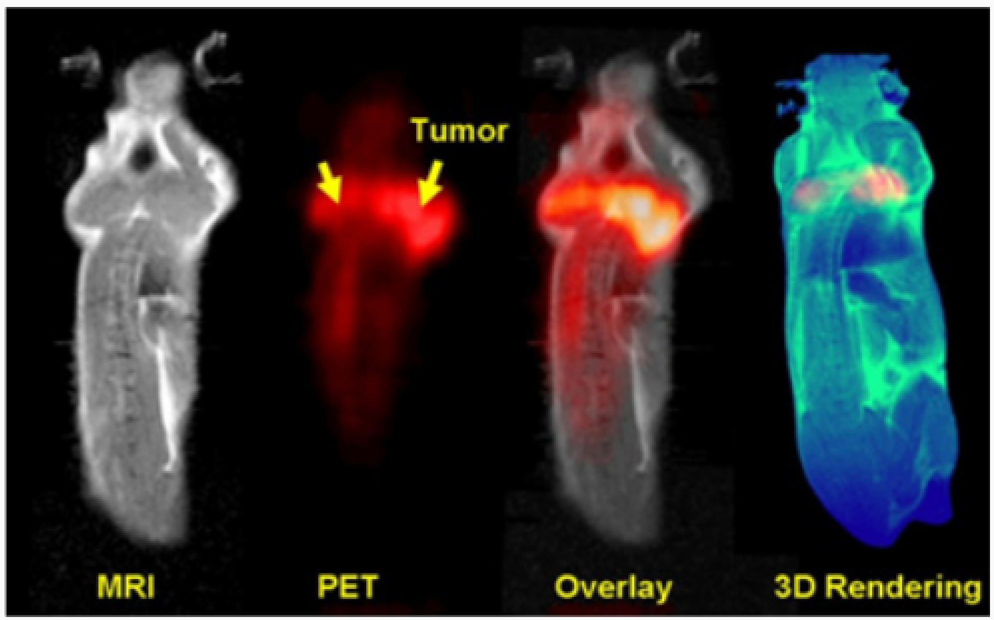

With the recent achievements in PET/MRI scanner technology, the use of radio-manganese, a manganese compound (i.e. a mixture of ^{52g}Mn and ^{51}Mn), may enable future dual modal imaging techniques, having both properties for MRI and PET.

Feasibility study: INFN project **METRICS** (CSN5).

Nuclear reaction theory: phenomenology

Overview of reaction components

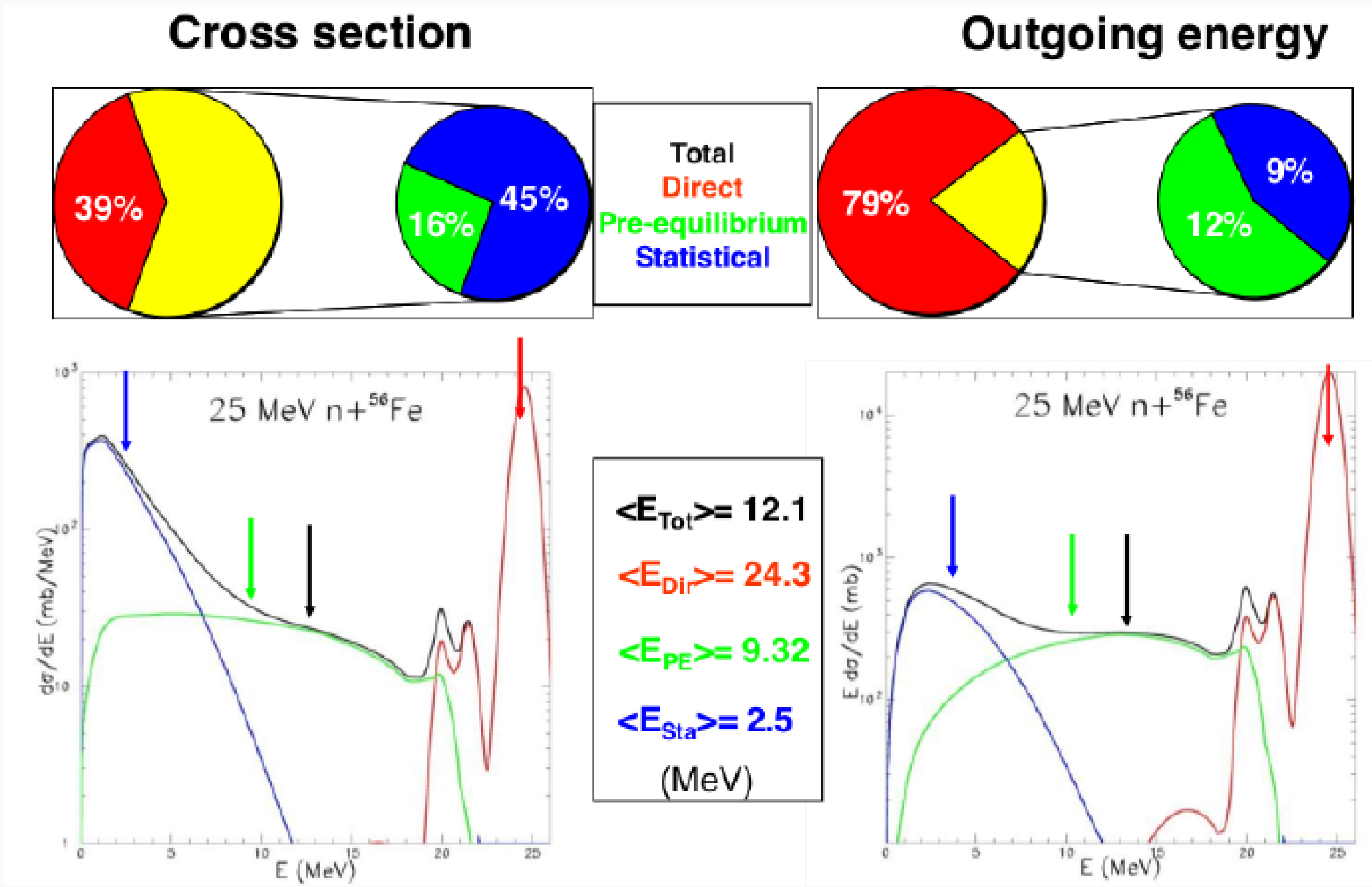

The problem to work with enriched targets!

Less tan 0.5 gram (49Ti & 50Ti)   27,3 Keuro

- HIVIPP method works with metal powders.. but we received metal sponges of ^{49}Ti and ^{50}Ti !

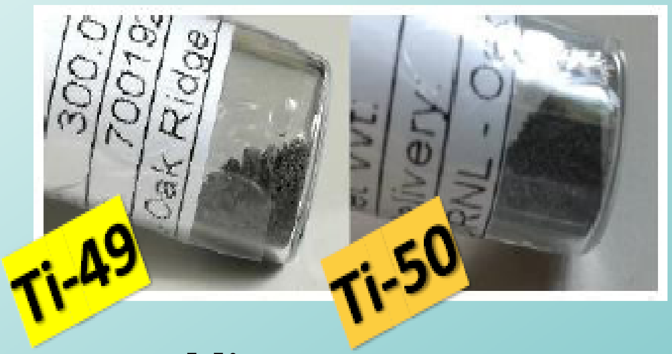

A. Skliarova, LNL

HIVIPP test

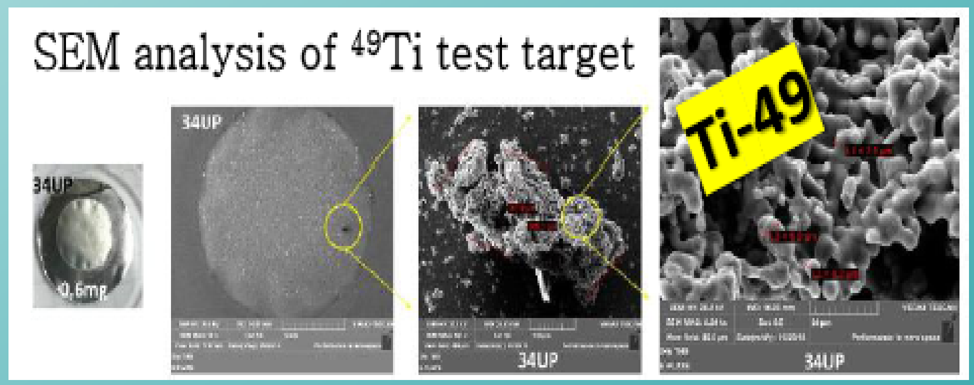

- Manual test with liquid N_2 to reduce the grains of ^{49}Ti into metal powder; HIVIPP deposition and analysis:

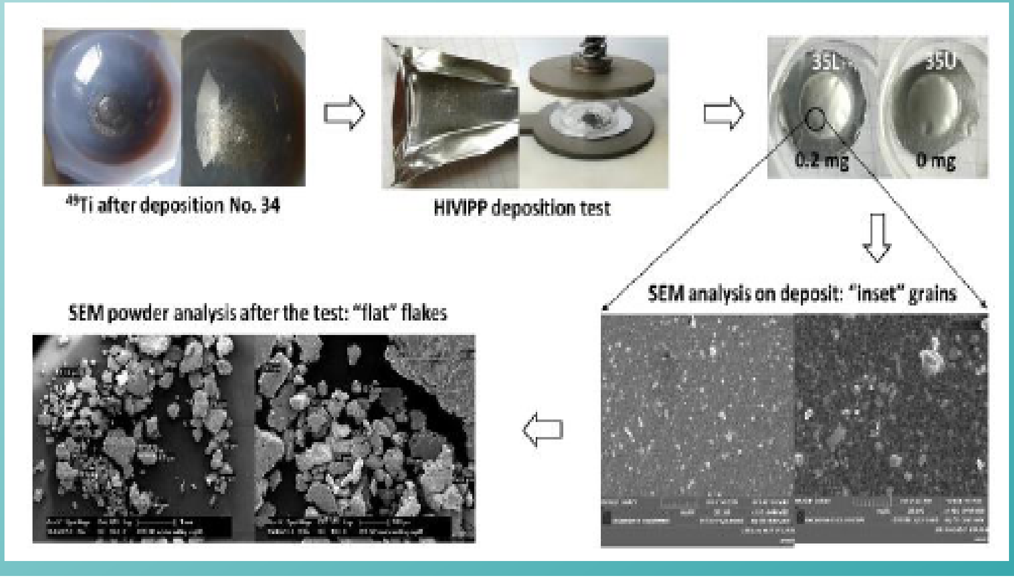

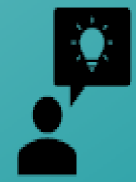

The positive outcomes encouraged the use of a **cryomill**, that is able to apply a multidirectional effect on the powder, thanks to a mechanical and vibrational movement.